Food and Agriculture Organization of the United Nations

General Fisheries Commission for the Mediterranean

JASCO APPLIED SCIENCES

Acoustic footprint of bottom trawling in the Adriatic Sea

Durrës, Albania

26 August–2 September 2023

By
Calder Robinson
Federica Pace
Özkan Sertlek

This study was conducted within the framework of the "Fisheries and ecosystem-based management for the blue economy of the Mediterranean" (FishEBM-MED) project. Funded by the Global Environment Facility (GEF), the FishEBM-MED project is implemented by the Food and Agriculture Organization of the United Nations (FAO) and the United Nations Environment Programme (UNEP), with execution overseen by the General Fisheries Commission for the Mediterranean (GFCM) and the Mediterranean Action Plan|SPA/RAC.

gef

Acknowledgments: The GFCM Secretariat and the authors of this study warmly thank Arian Palluqi for his invaluable contributions, including the preparation and planning of the study, the facilitation of fieldwork, and his continuous support.

Contents

Figures

Tables

Executive Summary

JASCO Applied Sciences (Deutschland) GmbH collaborated with the General Fisheries Commission for the Mediterranean to perform a Sound Source Characterisation (SSC) study of representative fishing activity in the Adriatic Sea off the coast of Durrës, Albania. The study was funded by Global Environmental Facility and took place in August 2023; it consisted of recording underwater sound radiated by a bottom trawler vessel before and during typical fishing operations. The aim of the measurements was to increase the scarce publicly available data on sound emissions from fishing vessels, and to enable more accurate modelling of noise impacts from fishing activities involving single or multiple boats near ecologically sensitive locations. To that end, from the analysis of the recorded data, the spectral source level of the vessel was to be computed so it could be used to improve the realism and accuracy of future modelling. In 2021 JASCO had performed such a numerical modelling study of fishing operations in the Adriatic at the Pomo/Jabuka Pit Fisheries Restricted Area, which had evidenced the scarcity of available sound levels data for fishing vessels engaged in their work.

The field campaign took place on 31 August 2023 and successfully captured on two digital recorders about two hours of acoustic signals from a bottom trawler performing a scripted series of activities. Only when the data were processed an anomaly was discovered that made the upper frequencies (above about 800 Hz) unsuitable for analysis. The procedure for deriving vessel source levels from selected portions of the recordings was otherwise successful and yielded a reliable source level spectrum for the vessel in phases of transiting, bottom trawling, and retrieving its gear – albeit only for frequency bands between 10 and 800 Hz. The derived source levels were found to be consistent with those of similar vessels engaged in trawling and showed that the source level estimation assumptions used for the 2021 study (Pace et al. 2023) had been realistic.

The last part of the study consisted of using the source levels obtained from the field measurements to conduct forward modelling of the sound from the vessel, that is, numerically estimate the propagation of its sound in regions altogether different from where it had been characterised to assess the potential impact on marine species. This modelling showed that despite the truncated frequency range the measurements-based source levels contained a large enough proportion of the acoustic energy to enable useful estimation of behavioural threshold ranges in the relevant regions.

Like in the 2021 study (Pace et al. 2023), underwater sound fields were modelled at six different locations for vessels employing set longlines (LLS) and otter-board trawls (OTB), with each vessel type split into small, medium, and large categories. Source levels for the OTB categories were updated using the SSC results to augment the original model-based estimates, yielding broadband monopole source levels for the small, medium, and large OTB vessels of 174, 176, and 178 dB re 1 µPa·m over the frequency range 10Hz-25kHz respectively.

Estimated underwater sound fields were calculated for sound pressure levels (SPL) to compare with established impact criteria for fish and marine mammals. The SPL thresholds for recoverable injury and temporary hearing threshold shift (TTS) in pressure sensitive fish from Popper et al. (2014) of 170 and 158 dB re 1 µPa respectively were not reached for any vessel at any location within the resolution of the modelling. The maximum modelled range to the behavioural response threshold for marine mammals from NOAA (2019) of 120 dB re 1 µPa was 0.94 km. Two multiple vessel scenarios were modelled based on realistic fishing schedules: Scenario 1 involved Croatian OTB vessels operating in Zone C and a mixture of Italian vessels in Zone B and Scenario 2 involved Croatian LLS vessels operating in Zone C and a mixture of Italian vessels in Zone B. Since estimated source levels for OTB vessels were significantly higher than those for LLS vessels, the overall ensonification resulted higher in Scenario 1 than Scenario 2.

1. Introduction

JASCO Applied Sciences (Deutschland) GmbH (JASCO) in collaboration with the General Fisheries Commission for the Mediterranean Sea (GFCM) carried out a Sound Source Characterisation (SSC) study of representative fishing activity in the Adriatic Sea off the coast of Durres, Albania (Figure 1).

The study, funded by Global Environmental Facility (GEF), took place in August 2023 and consisted of recording underwater sound emissions from a bottom trawler before and during typical fishing operations. The SSC measurements are aimed at increasing the amount of publicly available data on the sound emissions from fishing vessels.

In 2021, JASCO had carried out a noise modelling study on the potential effects of underwater noise on demersal fisheries on behalf of GFCM; the study highlighted the gap in publicly available data on the source levels of fishing vessels, especially when they are engaged in fishing activity as opposed to transiting (Pace et al. 2023). The lack of reliable source level data increases the uncertainty of modelling potential impacts of these type of vessels on marine life.

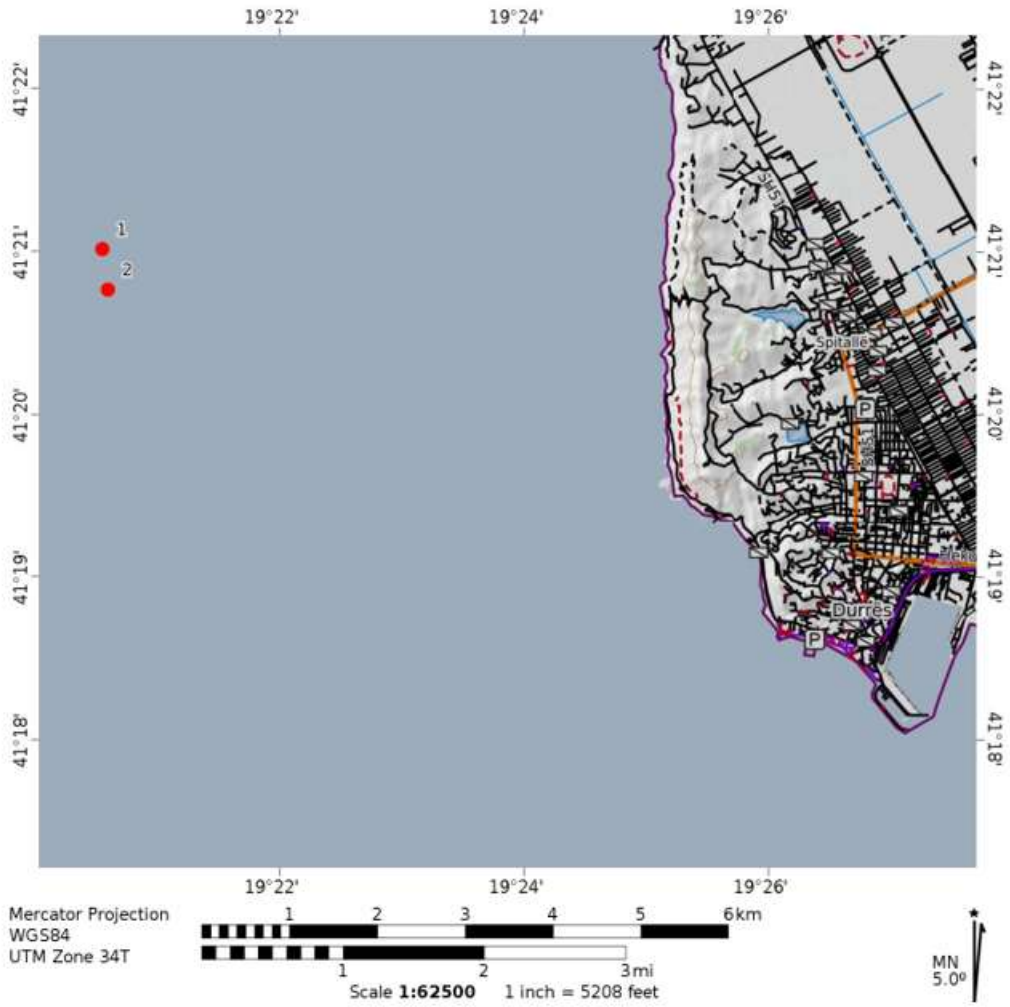

Figure 1. Map showing deployment location in relation to the nearby port of Durres, Albania

1.1. Ambient Sound

The acoustic environment of a location is known as its soundscape. A soundscape is comprised of the cumulative contributions from abiotic (geophonic), biotic (biophonic), and human (anthrophonic) sound sources (Krause 2008). Ambient sound is defined as any sound present in the absence of human activity. It is also temporally and spatially specific (ISO 2017a). The Wenz (1962) curves in Figure 2 show the typical frequencies and spectral levels of many of these activities.

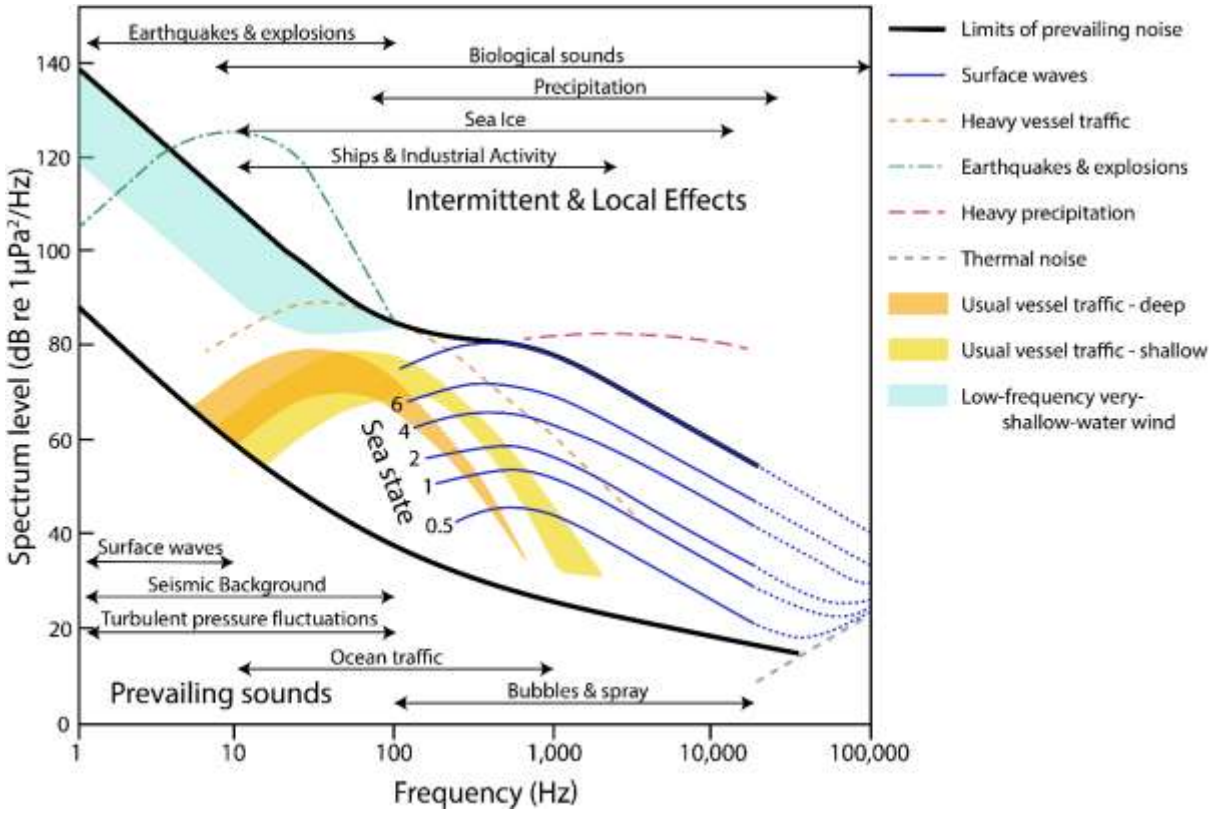

Figure 2. Wenz curves describing pressure spectral density levels of marine ambient sound from weather, wind, geologic activity, and commercial shipping (adapted from NRC 2003, based on Wenz 1962). The thick lines are the limits of prevailing ambient sound, which are included in some of the results plots to provide context.

In the marine environment, the geophonic elements of a soundscape can act as proxies for oceanographic conditions. Knudsen et al. (1948) and Wenz (1962) demonstrated that increased sea state and wind speed commonly correlate with higher sound intensities across frequencies from 500 Hz to 30 kHz due to breaking whitecaps, surface flow noise, wave generation, cavitation, and pressure change (Urick 1983). Rainfall can elevate sound levels in the 1–15 kHz frequency range via sound from surface impacts and bubble entrainment (Heindsmann et al. 1955, Bom 1969, Scrimger et al. 1987). Waves, sea ice, currents, and seismic activity (such as earth movement and subsea landslides) can also be loud, though short-duration, geophonic contributors. While geophonic and biophonic contributors comprise the natural soundscape, the total soundscape also includes anthrophonic (related to human activity) sounds.

Measuring ambient sound and characterizing the soundscape of an area is complicated by non-acoustic processes that often appear in acoustic recordings. One such issue is flow noise, which is caused by pressure eddies and vortices produced by water moving along the surfaces of hydrophone pressure transducers. This is similar to the buffeting sounds recorded by microphones in the wind. Flow noise is not part of a marine soundscape (Strasberg 1979, Urick 1983), but its intensity may

indicate current strength (Willis and Dietz 1961). Current or wave action can also induce mooring noise when non-stationary components of a mooring create sound as they move or strum.

1.2. Anthropogenic Contributors to the Soundscape

Anthropogenic (human-generated) sound can be a by-product of vessel operations, such as engine sound radiating through vessel hulls and cavitating propulsion systems, or it can be a product of active acoustic data collection with seismic surveys, military sonar, and depth sounding as the main contributors. Marine construction projects often involve nearshore blasting and pile driving that can produce high levels of impulsive-type noise. The contribution of anthropogenic sources to the ocean soundscape has increased from the 1950s to 2010, largely driven by greater maritime shipping traffic (Ross 1976, Andrew et al. 2011). Recent trends suggest that global sound levels are levelling off or potentially decreasing in some areas (Andrew et al. 2011, Miksis-Olds and Nichols 2016). Oil and gas exploration with seismic airguns, marine pile driving, and oil and gas production platforms elevate sound levels over radii of 10 to 1000 km when present (Bailey et al. 2010, Miksis-Olds and Nichols 2016, Delarue et al. 2018).The extent of seismic survey sounds has increased substantially following the expansion of oil and gas exploration into deep water, and seismic sounds can now be detected across ocean basins (Nieukirk et al. 2004).

1.2.1. Vessel Traffic

There are some major shipping lanes in the study area (Figure 3), most notably those heading west and northwest out of the Port of Durres associated with ferry traffic to/from Italy. In addition to the major shipping lanes is a high density of near short vessel activity, attributed primarily to intercoastal traffic and fishing activity, like that of interest in this study. Vessel fan out after leaving the Port of Durres, resulting in consistent traffic in region.

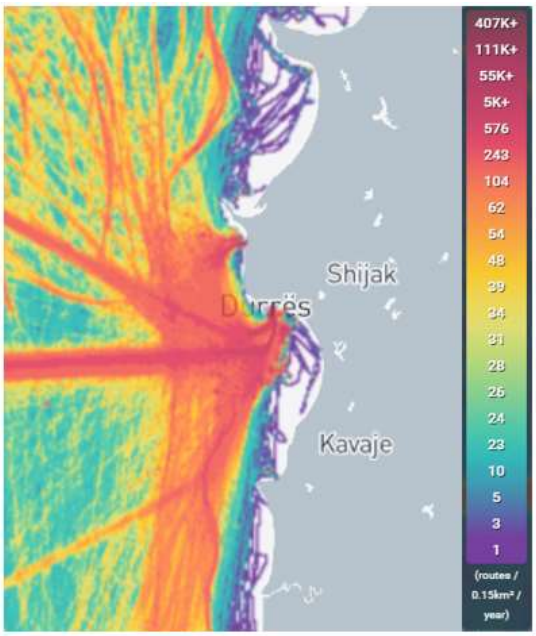

Figure 3. 2022 vessel traffic density off the coast of Albania in the study area (source: marinetraffic.com; accessed 16 January 2024). Colour indicates relative density of shipping tracks over the preceding year

2. Methods

The following sections detail the Acoustic data collection and subsequent analysis that was used to estimate the source level of fishing vessels in this region of Adriatic. Section 2.1 provides specifications of the hydrophones and recording set-ups used to record audio throughout the trial. Section 2.2 provides and overview of the other non-acoustic data collected during the trial that was used in estimating the source level, including GPS tracks, an activity log, and CTD casts. Section 2.3 discusses the calculation of acoustic metrics used to quantify the sound scape, the specific source level of the vessel, and estimation of its impact.

2.1. Acoustic Data Acquisition

On the 31st of August, JASCO deployed two Autonomous Multichannel Acoustic Recorders (AMARs) Generation 4 (G4), also manufactured by JASCO, to measure SPL produced by the fishing vessel *Rozafa 11*. The AMARs, in a baseplate configuration (Figure 4) fitted with an M36 omnidirectional hydrophone (GeoSpectrum Technologies Inc., -165 ± 3 dB re 1 V/µPa sensitivity), were deployed at the 2 locations shown in Figure 1 for just over 10 hours (Table 1). The hydrophones were protected by a hydrophone cage, which was covered with an open-cell foam fairing and a Lycra shroud to minimize non-acoustic noise, or 'flow noise', caused by water flowing over the hydrophone transducer (Cotter et al. 2024). The AMARs recorded continuously at 128 kHz for a usable recording bandwidth of 10 Hz to 64 kHz. Acoustic data were stored on 512 Gb of internal solid-state flash memory. The full recording chain (recorder fitted with the selected hydrophone) was calibrated prior to deployment and after retrieval, in line with best practice guidelines (Robinson et al. 2014), as described in Appendix A. The AMARs were retrieved as planned using acoustic releases.

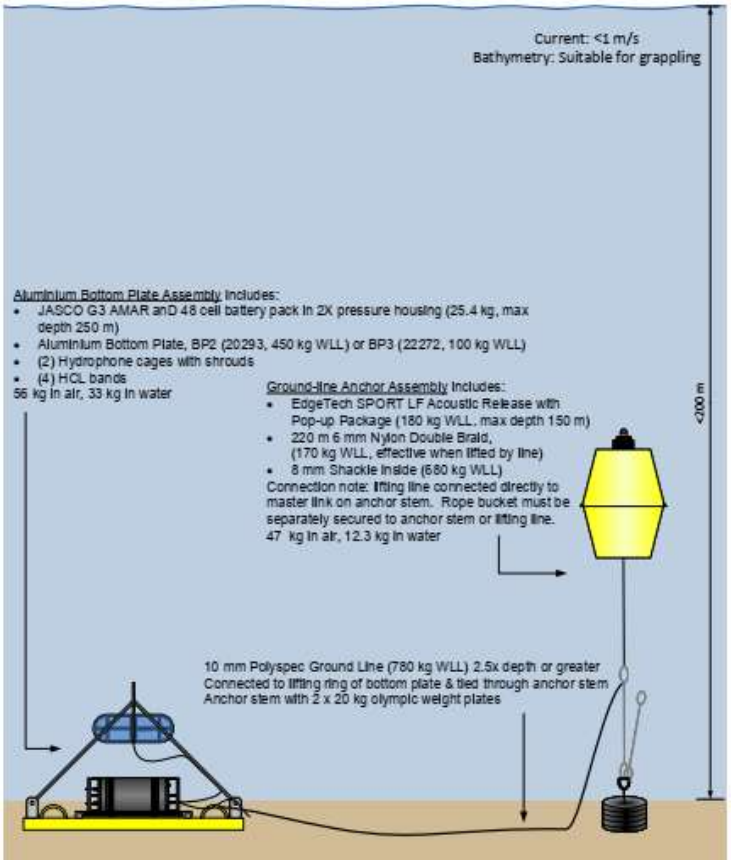

Figure 4. Deployment configuration of the AMAR. This configuration was replicated at each deployment location.

Table 1. Operation period, location, and water depth of the AMARs deployed for the Sound Source Characterization study. All recordings took place on 2023-08-31.

Station	Latitude (°N)	Longitude (°E)	Depth (m)	Deployment	Retrieval	Duration (Hours)
1	41.35018	19.342617	63	09:24	18:00	10:46
2	41.34605	19.343387	61	08:23	17:25	10:15

2.2. Other Data Acquisition

In addition to acoustic data, environmental data and information about the vessel, tracks, and fishing activity were recorded throughout the study. The *Rozafa 11* (Figure 5, Table 2), the primary vessel of interest, is a 120-ton fishing vessel which typically conducts fishing activity using benthic and pelagic trawls.

Figure 5. Fishing Vessel *Rozafa 11* viewed while transiting. Image provided by Rozafa Ltd.

Table 2. Source vessel characteristics.

Vessel name	IMO number	LOA (m)	Draft (m)	Source depth (m)
Rozafa 11	86616113	25.5	2.8	2

GPS tracks were collected for the vessel using a hand-held GPS unit during transiting, deployment, trawling and retrieval activities. This track was used to calculate the separation between vessel and receiver necessary for source level calculation. Figure 6 provides a map of the GPS tracks used in the calculations. GPS closest point of approach (CPA) and acoustic CPA were aligned in time prior to performing separation and source level calculations.

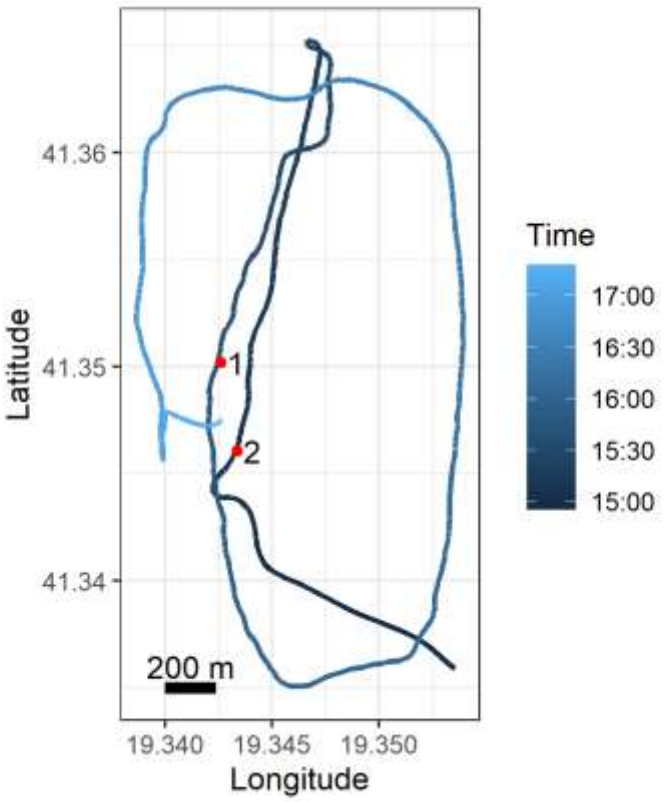

Figure 6. GPS track of *Rozafa 11* in relation to the two recording stations.

In addition to the GPS tracks, JASCO personnel on board recorded a time-based activity log which was used to identify the acoustic characteristics of the different fishing activities. A condensed form of the log is available in Table 3 and the full log is available in Appendix B.

Table 3. Condensed activity log used to identify different activity signatures in later analysis. All activities took place on 31 Aug 2023.

Vessel Activity	Start Time (UTC)	End Time UTC
Pass 1	14:55	15:20
Pass 2	15:22	15:54
Deploy	16:04	16:11
Trawl	16:12	17:02
Retrieve	17:02	17:12

2.2.1. CTD Casts

Collaborating partners measured oceanic parameters that impact underwater sound propagation using a CTD the morning of the trial. Figure 7 shows key parameters by depth, including the temperature, salinity, density, and sound velocity profiles.

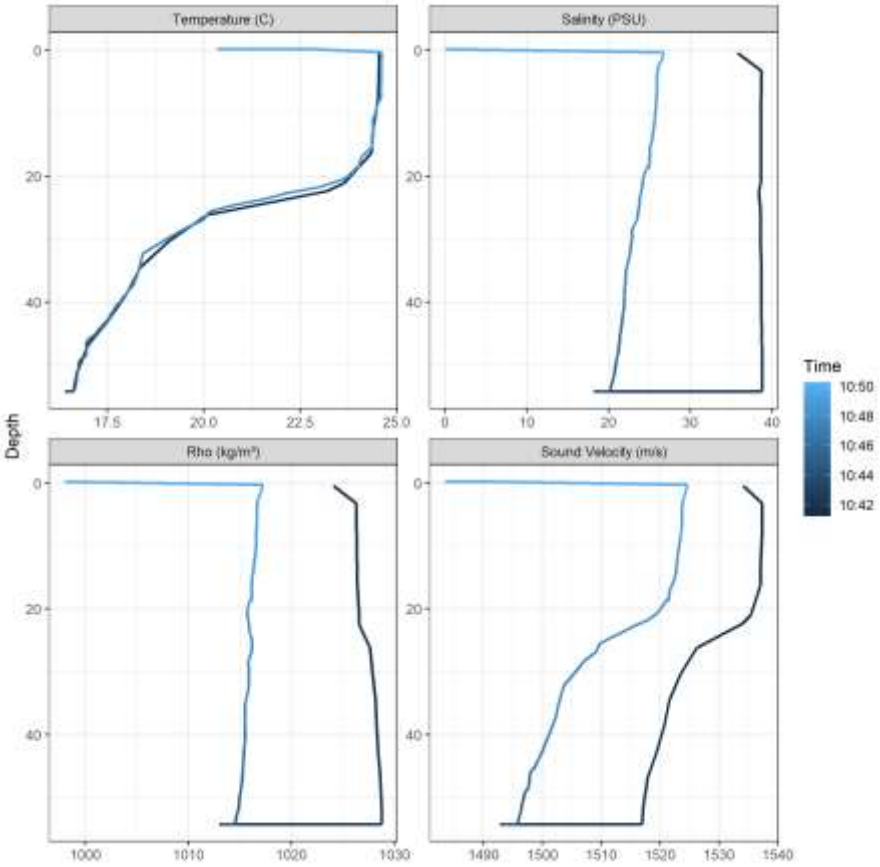

Figure 7. Depth profiles of the various CTD parameters, taken on 2023-08-31 between 10:40 and 10:50. Surface is at the top of the profile. The horizontal portions of the profiles are non-physical and represent the device pausing at a given depth.

2.3. Data Analysis

The following sections describe the processing chain used to estimate the vessel source level and determine the scope of potential impacts on the environment. Section 2.3.1 describes the automated data processing that was applied to the entire data set to provide standardized acoustic metrics to quantify the ambient sound in the region, as well as feed into following steps. Section 2.3.2 details the manual selection of data from the automated analysis according to the time stamp and log of operations to identify the data corresponding to the individual vessel passes and activities of interest, before being used to calculate the source level (SL).

2.3.1. Ambient Data Analysis

The goal of the total ocean sound analysis is to present this data set in a manner that documents the baseline underwater sound conditions in the Adriatic, off the coast from Durrës. The first stage of the total sound level analysis involves computing the peak sound pressure level (PK) and sound pressure level (SPL) for each minute of data. This reduces the data to a manageable size without compromising its value for characterizing the soundscape (ISO 2017b, Ainslie et al. 2018, Martin et al. 2019). SPL analysis was performed by averaging 120 fast-Fourier transforms (FFTs) that each included 1 s of data with a 50 % overlap that use the Hann window to reduce spectral leakage. The 1 min average data were stored as power spectral densities (1 Hz resolution up to 455 Hz and millidecades frequency

bands above 455 Hz) and summed over frequency to calculate decidecade band SPL (decidecade band levels are similar to 1/3-octave-band levels.)

The millidecade band analysis approach described in Martin et al. (2021) was also applied to the data. Millidecades are logarithmically spaced frequency bands but have a bandwidth equal to 1/1000th of a decade. Using millidecades instead of 1 Hz frequency bands reduced the size of the spectral data by a large factor without compromising the usefulness of the data.

The decidecade analysis sums as many frequencies as contained in the recorded bandwidth in the power spectral density data to a manageable set of up to 45 bands that approximate the critical bandwidths of mammal hearing. The decade bands further summarize the sound levels into four frequency bands for manageability. Appendices C.1 and C.2 contain detailed descriptions of the acoustic metrics and decidecade analysis, respectively.

In section 3.1, the total sound levels are presented as:

- **Band-level plots**: These strip charts show the averaged received SPL as a function of time within a given frequency band, including the total sound levels across the entire recorded bandwidth (10–16,000 Hz) and the levels in the decade bands of 8.9–89.1 Hz (Decade A); 89.1–891.3 Hz (Decade B); 891.3–8,913 Hz (Decade C); and 8,913–16,000 Hz (Decade D), depending on the recording bandwidth. The 8.9–89.1 Hz band is generally associated with fin and blue whales, large shipping vessels, flow and mooring noise, and seismic survey impulses. Sounds within the 89.1–891.3 Hz band are generally associated with the physical environment such as wind and wave conditions but can also include both biological and anthropogenic sources such as minke and humpback whales, fish, smaller vessels, seismic surveys, and pile driving. Sounds above 1000 Hz include high-frequency components of humpback whale sounds, odontocete whistles and echolocation signals, wind- and wave-generated sounds, and sounds from human sources at close range including pile driving, vessels, seismic surveys, and sonars.
- **Long-term Spectral Averages (LTSAs)**: These colour plots show power spectral density levels as a function of time (*x* axis) and frequency (*y* axis). The frequency axis uses a logarithmic scale, which provides equal vertical space for each decade increase in frequency and equally shows the contributions of low- and high-frequency sound sources. The LTSAs are excellent summaries of the temporal and frequency variability in the data.
- **Decidecade box-and-whisker plots**: The ‘boxes’ in these figures represent the middle 50 % of the range of SPL, so that the bottom of the box is the sound level 25th percentile (L_{25}) of the recorded levels, the bar in the middle of the box is the median (L_{50}), and the top of the box is the level that exceeded 75 % of the data (L_{75}). The whiskers indicate the maximum and minimum ranges of the data.
- **Spectral density level percentiles**: While the decidecade box-and-whisker plots represent the histogram of each band’s sound pressure levels, the power spectral density data have too many frequency bins for a similar presentation. Instead, coloured lines represent the L_{eq}, L_5, L_{25}, L_{50}, L_{75}, and L_{95} percentiles of the histograms. Shading underneath these lines indicate the relative probability distribution. It is common to compare the power spectral densities to the results from Wenz (1962), which documented the variability of ambient spectral levels off the US Pacific coast as a function of frequency of measurements for a range of weather, vessel traffic, and geologic conditions (see Figure 2). The Wenz levels are only appropriate for approximate comparisons because those data were collected in deep water, largely before an increase in low-frequency sound levels (Andrew et al. 2011).

2.3.2. Vessel Data Analysis

Using the JASCO acoustic analysis software PAMlab (see Appendix C), and referring to the activity log of the *Rozafa 11* (Table 3, Appendix B) for the timing of relevant operations, segments of the acoustic recordings corresponding to the passage of the vessel past the monitoring stations were identified and selected. Features of the sound attributable to extraneous sources whether biological (e.g. snapping shrimp) or anthropogenic (e.g. large vessels transiting at farther range) were flagged so they could be excluded from the sound level analysis. The characteristic signature pattern of the target vessel approaching and moving past a station, as visualised in a spectrogram display (see Section 3.2.1), enabled the precise determination of the time-distance relation between source and receiver that would be used in the estimation of source levels.

2.4. Estimating Ranges to Acoustic Thresholds

Estimating ranges to acoustic thresholds of impact on marine life required firstly to estimate the source levels based on the field measurements (back-propagation, as explained in Section 2.4.1), and then to forward propagate the signals spectra to determine the received levels at specified ranges from the source (for multiple depths) for each of the vessels considered in the study, as described in Section 2.4.2. Furthermore, modelling was performed for sound fields comprising multiple vessels to represent two realistic scenarios of the potential disturbance of sounds from fishing activity on marine receptors (2.4.3).

2.4.1. Vessel Source Level Estimation

Source Level (SL) is the sound level at a reference distance from the sound source, typically 1 m. To compute SL from the Received Level (RL), the sound recorded by a receiver, the distance between the sound source and the receiver as well absorption in the wave guide must be accounted for. Following the ISO 17208-1:2016 reference method, the RL is standardized by range into Radiated Noise Level (RNL) with the following formula:

$$RNL = RL + 20 \times \log_{10} R$$

Where RNL and RL are defined above, and R is the distance between the source and the receiver, in meters, calculated sing time synchronized GPS tracks. The RNL is then used to calculate SL by applying frequency dependant absorption and seabed reflection corrections (Ainslie et al. 2022). Data within the 30° azimuth window of a passing vessel are averaged to provide the 1s, decidecade source level. In this study, SL level was computed for the vessel under normal transiting conditions, trawling conditions, and equipment retrieval. SL for Deployment was not computed as it occurred too far away from the receiver.

2.4.2. Sound Level Forward Modelling

In the 2021 modelling study, spectral source levels estimated for different types of fishing vessels were used as input to a propagation model to assess the ranges at which various noise effects thresholds for marine life present in the region might be exceeded. Having experimentally obtained source levels for one type of fishing vessel in the current SSC study, those previous ranges can now be revisited in comparison. Six source locations (Table 4) had been considered for the modelling, shown on a map in Figure 8 relative to the zones of the Pomo/Jabuka Pit Fisheries Restricted Area (FRA) whereby fishing is forbidden in Zone A and only permitted in Zones B and C subject to regulatory restrictions imposed by Italy and Croatia respectively.

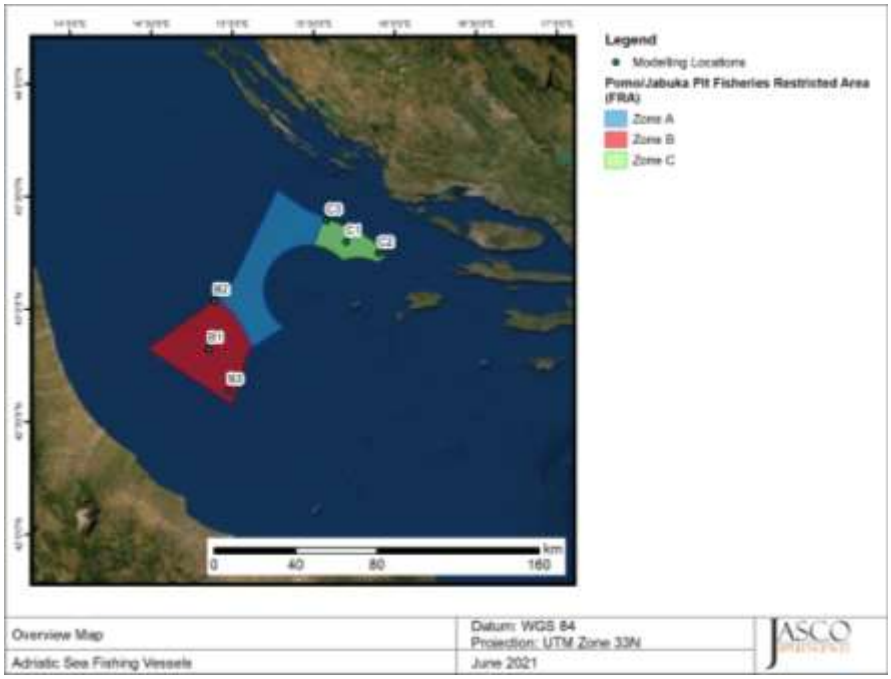

Figure 8. A map of the modelled area showing the Zones of the FRA and the modelling locations.

Table 4. List of modelling locations in Zones B and C of the Pomo/Jabuka Pit Fisheries Restricted Area.

Zone	Site name	Description	Latitude	Longitude	UTM (WGS84), Zone 33 N		Water depth (m)
					Easting (m)	Northing (m)	
B	B1	Zone centre	42° 49' 45.8" N	14° 51' 25.4" E	488317	4741878	227.0
	B2	Zone shallow point	43° 02' 34.7" N	14° 53' 18.1" E	490906	4765593	127.4
	B3	Zone mid-depth point	42° 38' 41.0" N	14° 58' 27.8" E	497900	4721364	200.0
C	C1	Zone centre	43° 18' 10.4" N	15° 41' 24.2" E	555969	4794683	137.3
	C2	Zone shallow point	43° 14' 58.2" N	15° 52' 59.7" E	571700	4788900	124.2
	C3	Zone deep point	43° 23' 50.1" N	15° 34' 22.0" E	546385	4805089	181.6

The notional source depth of the subject vessel in the SSC study, the *Rozafa 11*, matches that of the proxy vessel for one of the categories (OTB-M, meaning otter-board bottom trawler of medium size) modelled in 2021; this enables the reuse of the propagation loss data computed for that category in the earlier study to estimate corresponding received levels from the new source levels data. Overall similarities in other properties (Table 5) make it meaningful to draw a comparison between the threshold effect ranges estimated for the two.

Table 5. Comparison of vessel properties for a proxy in the 2021 study and the vessel measured in 2023.

Vessel category	Vessel	LOA (m)	Draft (m)	Source depth (m)
OTB-M	*Princeza Grejn*	20.2	3.2	2.1
	Rozafa 11	25.5	2.8	2.0

To estimate received sound levels at increasing distances from the source in all directions, from which ranges to relevant threshold levels for potential effects on marine fauna would be computed, the same propagation modelling approach (see Appendix D) and parametrisation (see Figure 9, Table 6 and Table 7) were used as in the 2021 study. As described in that earlier study, the modelled sites were divided into two geoacoustic areas based on the water depth at the source. Sites with a water depth greater than 150 m were categorised as an organic clay-loam substrate (here modelled as calcareous

silt-clay), while sites with a water depth shallower than 150 m were categorised as a terrigenous sand-silt-clay, based on information provided by GFCM and the EMODnet Seabed Substrate map. A mean monthly water sound speed profile for the month of June was used at the request of GFCM.

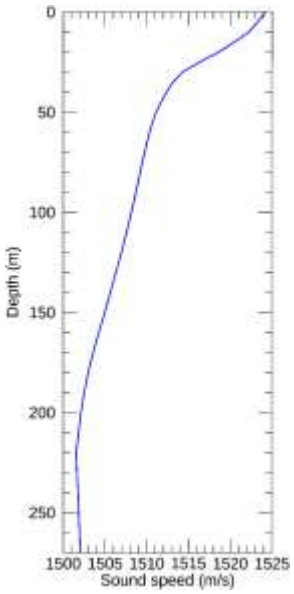

Figure 9. Mean monthly sound speed profile for June derived from data obtained from *GDEM V 3.0*.

Table 6. Estimated geoacoustic profile for Sites B1, B3, and C3 (water depth at source >150 m). Within each depth range, each parameter varies linearly within the stated range.

Depth below seafloor (m)	Material	Density (g/cm³)	Compressional Wave		Shear Wave	
			Speed (m/s)	Attenuation (dB/λ)	Speed (m/s)	Attenuation (dB/λ)
0.0-62.5	Silt-clay	1.40-1.51	1510-1610	0.17-0.21	116	2.00
62.5-125.0		1.51-1.60	1610-1710	0.21-0.35		
125.0-187.5		1.60-1.67	1710-1810	0.35-0.73		
187.5-250.0		1.67-1.72	1810-1910	0.73-1.07		
250.0-312.5		1.72-1.76	1910-2010	1.07-1.38		
312.5-375.5		1.76-1.80	2010-2100	1.38-1.64		
375.0-437.5		1.80-1.83	2100-2200	1.64-1.50		
437.5-500.0		1.83-1.86	2200-2270	1.50-1.35		

Table 7. Estimated geoacoustic profile for Sites B2, C1, and C2 (water depth at source <150 m). Within each depth range, each parameter varies linearly within the stated range.

Depth below seafloor (m)	Material	Density (g/cm³)	Compressional Wave		Shear Wave	
			Speed (m/s)	Attenuation (dB/λ)	Speed (m/s)	Attenuation (dB/λ)
0.0-62.5	Sand-silt-clay	1.60-1.68	1550-1630	0.23-0.63	250	3.65
62.5-125.0		1.68-1.76	1630-1700	0.63-1.04		
125.0-187.5		1.76-1.83	1700-1770	1.04-1.32		
187.5-250.0		1.83-1.90	1770-1830	1.32-0.98		
250.0-312.5		1.90-1.97	1830-1890	0.98-0.92		
312.5-375.5		1.97-2.03	1890-1950	0.92-0.91		
375.0-437.5		2.03-2.09	1950-2000	0.91-0.89		
437.5-500.0		2.09-2.14	2000-2050	0.89-0.87		

2.4.3. Multiple Vessel Sound Fields

In the 2021 modelling study, six vessel types had been considered as sources for the estimation of sound fields for fishing fleet operations: set longlines (LLS) of three sizes and otter-board bottom trawlers (OTB) of three sizes. Their source level spectra had been estimated using the JOMOPANS-ECHO model (MacGillivray and de Jong, (2021) yielding the broadband source levels in Table 8.

Table 8. Modelled broadband monopole source levels for the various vessel categories.

Vessel category		Broadband MSL (dB re 1 µPa·m)
LLS	S	149.2
	M	151.4
	L	152.6
OTB	S	171.3
	M	173.4
	L	175.2

As explained in section 2.4.1, the source spectrum for the OTB-M category can be updated with the levels from the acoustic measurements of the trawler in the SSC study. For the other two OTB sizes, it was considered reasonable to assume the same spectral profile and offset the measurement-based OTB-M decidecade band levels by the difference between the modelled broadband source levels for the corresponding categories. No such assumption can be justified for the LLS categories because of the dissimilarities in vessels and operations between the two fisheries, so the modelled source spectra from the 2021 study were not modified.

The sound footprint for multiple vessels operating in the FRA zones simultaneously was estimated, like in the earlier study, by estimating the SPL footprint for each vessel type at the individual transmission loss modelling sites and then transposing and summing these footprints at various other locations within the zones. This method acceptably reflects large-scale sound propagation features, primarily dependent on water depth, which dominate the multiple source field, and is considered to provide a meaningful estimate of the sound field.

Two multiple vessel scenarios, identical to the ones used in the 2021 study, were assumed based on the local fishing regulations in Zones B and C. Scenario 1 represents a day where only OTB vessels are allowed to fish in Zone C, and Scenario 2 represents a day where only LLS are allowed to fish in Zone C; in both cases, conservative assumptions were made of the number of vessels that could be operating in each of the two Zones compatibly with regulations. A breakdown by type of the number of vessels modelled in each FRA zone is presented in Table 9; the source locations and the category of vessel modelled at each location for the two scenarios are presented in Appendix E.2.

Table 9. Summary of the vessel types modelled in each FRA zone for the two multiple vessel scenarios.

FRA Zone	Vessel category		Number of modelled vessels	
			Scenario 1	Scenario 2
B	LLS	S	0	0
		M	2	2
		L	3	3
	OTB	S	2	2
		M	6	6
		L	6	6
C*	LLS	S	–	11
		M	–	1
		L	–	0
	OTB	S	26	–
		M	13	–
		L	12	–

*The number of modelled vessels in Zone C represents the total number of vessels of each type authorised to fish in the region. This is a conservative estimate in the absence of any further information since not all vessels will necessarily operate within Zone C simultaneously.

3. Results

The following sections provide a comprehensive view of the results and acoustic metrics generated over the source of this study. Section 3.1 Describes the ambient sound in the regions, provides an overview of the entire deployment, and explains some of the common acoustic signatures visible in the data, including passing ships and the effects of bubble interference. Section 3.2.1 presents the results of the manual analysis of the vessel signatures during key fishing activities, including transiting, trawling, and retrieval of the fishing equipment. The representative vessel source level for each of these activities are also presented in this section. The final section, 3.3, provides the results of the sound source forward modelling, where estimated source levels are propagated through the environment to estimate ranges of effect.

3.1. Ambient Sound Analysis

The band-level plots, spectrograms (Long-term Spectral Averages), decidecade box-and-whisker plots, and spectral density level percentiles provide an overview of the sound variability in time and frequency presenting an overview of presence and level of contribution from different sources (Figure 10 and 11). Short-term events appear as vertical stripes on the spectrograms and spikes on the band level plots. Vessel signatures appear as V- and U-shaped artifacts stacked in frequency.

The sharp discontinuity in spectral levels occurring just below 1000 Hz at station 1 and 600 Hz at station 2 has been attributed to air bubbles trapped in the foam fairing installed on the hydrophone to mitigate flow noise, which acted as acoustic reflectors scattering the sound. In both records this effect is also observed as interference patterns (Annotation A) which drift upward in frequency over time as the bubbles slowly diffuse out of the foam.

The acoustic records show evidence of other ship traffic in the region, with annotations B and C denoting respectively nearby and distant shipping appearing in the spectrograms as V- and U-shaped features stacked in frequency. Annotations D and E in both figures identify times where source level analysis was performed on the subject vessel.

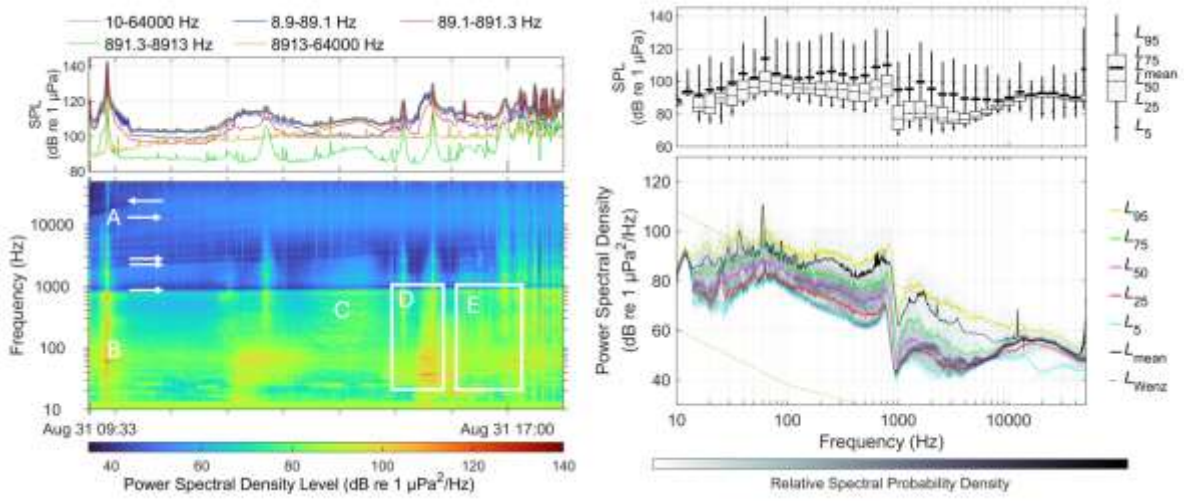

Figure 10. Ambient sound analysis at Station 1, 31 Aug 2023. Left) Band-level and long-term spectral averages throughout the deployment. Annotations show features of interest: A) Interference discontinuities caused by bubbles in the fairing, B) Close range ship transit, C) Distant ship transit, D) Two *Rozafa 11* Transits used in later analysis, E) Deployment, trawling, and retrieval used in later analysis. Right) Decidecade box-and-whisker plot and spectral density throughout the deployment.

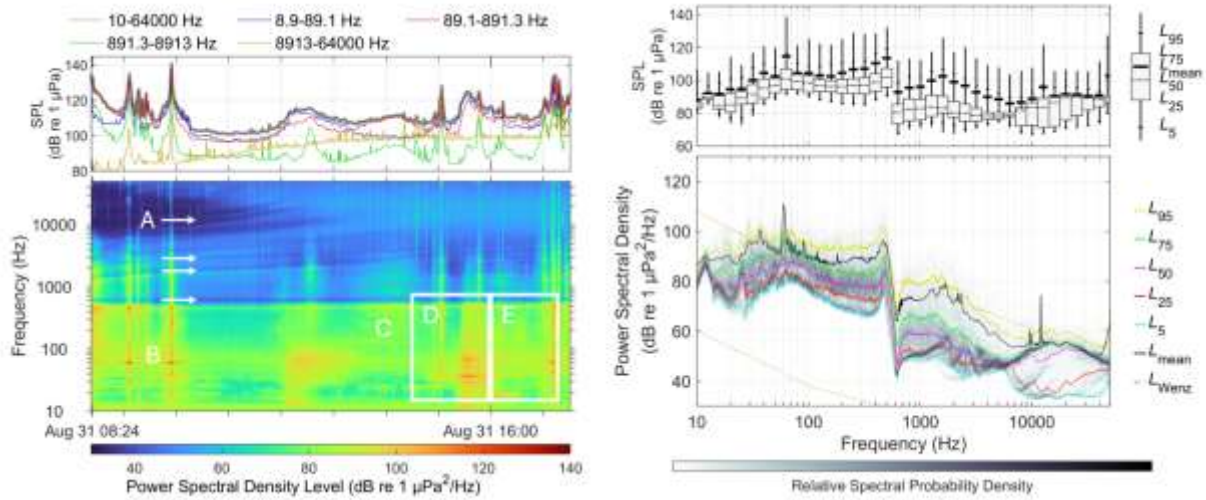

Figure 11. Ambient sound analysis at Station 2, 31 Aug 2023. Left) Band-level and long-term spectral averages throughout the deployment. Annotations show features of interest: A) Interference discontinuities caused by bubbles in the fairing, B) Close range ship transit, C) Distant ship transit, D) Two *Rozafa 11* Transits used in later analysis, E) Deployment, trawling, and retrieval used in later analysis. Right) Decidecade box-and-whisker plot and spectral density throughout the deployment.

Given the anomalous effect of trapped air bubbles on the acoustic recordings that was described above, unless otherwise stated all analyses and results that follow will be limited to frequencies up to 800 Hz for data from Station 1, and 600 Hz for data from Station 2.

3.2. Vessel Sound Analysis

3.2.1. Vessel Signature Identification

Figures 12 and 13 present the full-frequency spectrograms of the fishing vessel *Rozafa 11* passing respectively stations 1 and 2, while Figures 14 and 15 show the corresponding spectrograms truncated to the regions unaffected by the recording anomaly. The spectrograms clearly illustrate, as a vessel passes by the recorder (B), the Lloyd's mirror, or bathtub pattern caused by consecutive constructive and destructive interference between direct and reflected paths of sound as the path length difference moves through multiples of the wavelength at a given frequency. In these recordings the vessel did not have its fishing gear deployed and was simply transiting through the study area at a speed of 3-4 knots. The 50 kHz tone visible in the spectrogram (A) is emitted by the vessel echosounder; the lobe pattern observable at the time of CPA is attributable to the highly directional nature of this source. Other acoustic sources observable in the spectrogram include the high frequency snapping of shrimp (C) and a distant pass characteristic of a larger vessel (D).

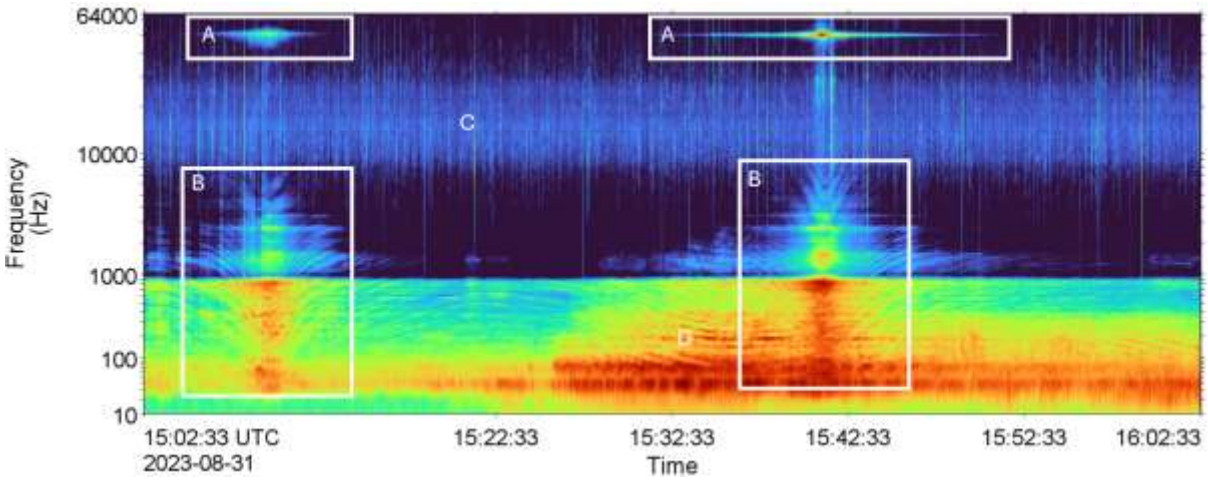

Figure 12. Vessel transit sound analysis of the *Rozafa 11* at Station 1, full band. Spectrogram of the acoustic record showing the Acoustic CPAs (B) of the vessels and the characteristic Lloyds mirror pattern. Signals at 50 kHz (A), are the depth sounders in operation onboard. Signals between 10 and 30 kHz (C) are likely snapping shrimp. D) is a distant pass characteristic of a larger vessel. Spectrogram has a frequency resolution of 2 Hz, a frame length of 0.125s, a timestep of 0.03125s, and Hamming window. Colour indicates relative intensity. The 25th and 99.99th percentile amplitude bounds are 61 and 118 dB re 1µPa/Hz respectively.

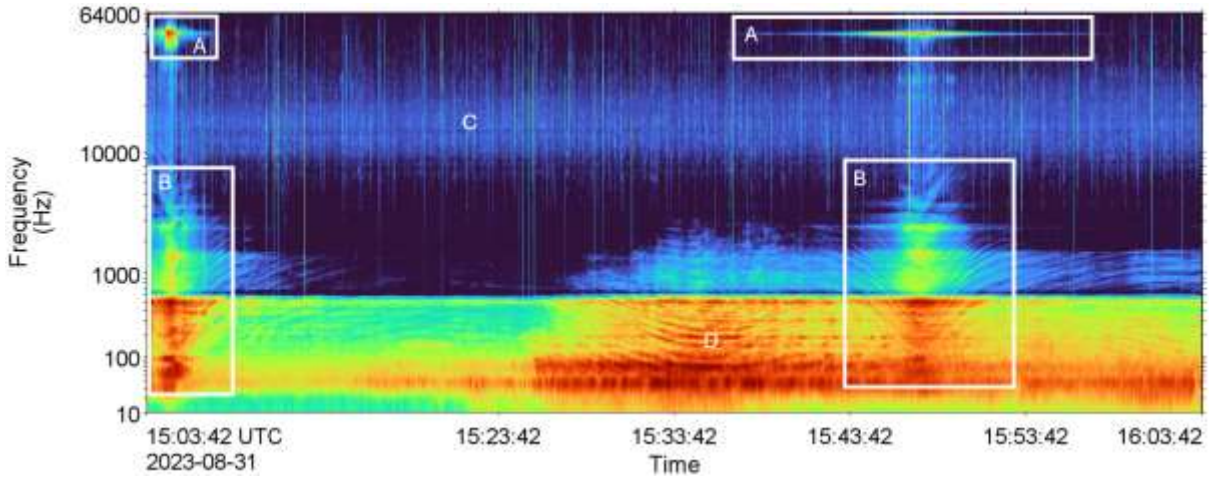

Figure 13. Vessel transit sound analysis of the *Rozafa 11* at Station 2, full band. Spectrogram of the acoustic record showing the Acoustic CPAs (B) of the vessels and the characteristic Lloyds mirror pattern. Signals at 50 kHz (A), are the depth sounders in operation onboard. Signals between 10 and 30 kHz (C) are likely snapping shrimp. D) is a distant pass characteristic of a larger vessel. Spectrogram has a frequency resolution of 2 Hz, a frame length of 0.125s, a timestep of 0.03125s, and Hamming window. Colour indicates relative intensity. The 25th and 99.99th percentile amplitude bounds are 61 and 115dB re 1µPa/Hz respectively.

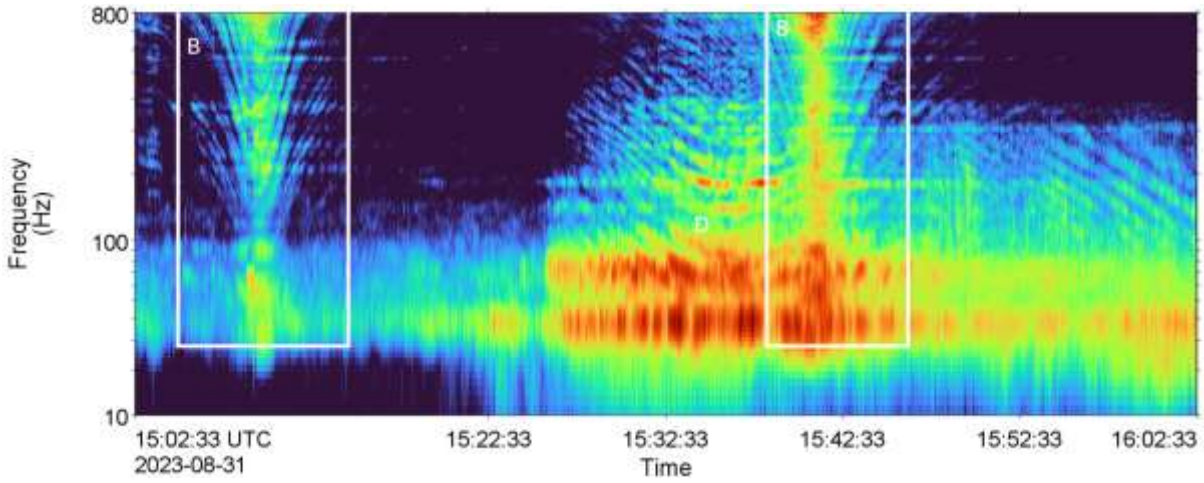

Figure 14. Vessel transit sound analysis of the *Rozafa 11* at Station 1, truncated band. Spectrogram of the acoustic record showing the Acoustic CPAs of the vessels (B) and the characteristic Lloyds mirror pattern. D) is a distant pass characteristic of a larger vessel. Spectrogram has a frequency resolution of 2 Hz, a frame length of 0.125s, a timestep of 0.03125s, and Hamming window. Colour indicates relative intensity. The 25th and 99.99th percentile amplitude bounds are 61 and 118 dB re 1µPa/Hz respectively.

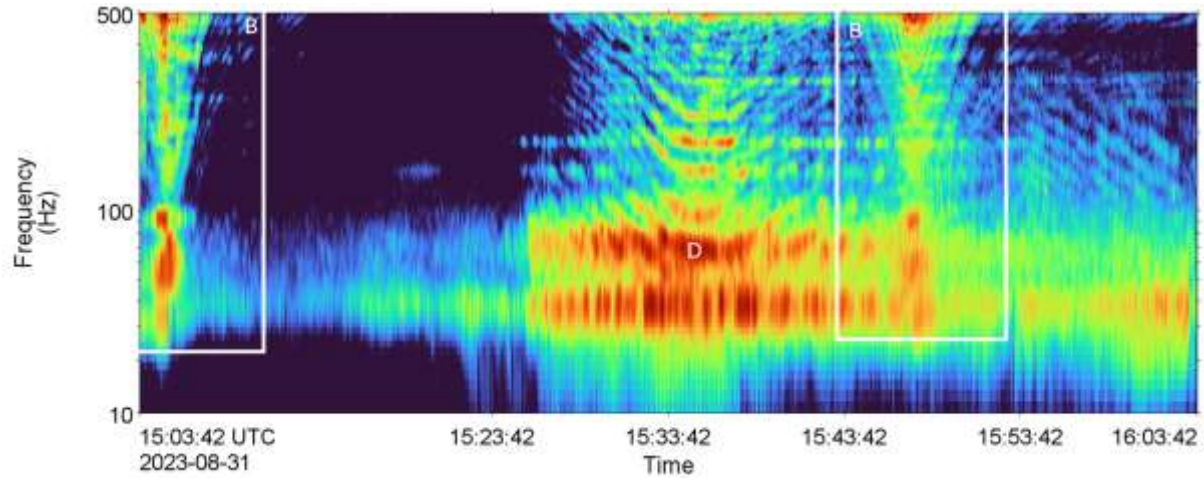

Figure 15. Vessel transit sound analysis of the *Rozafa 11* at Station 2, truncated band. Spectrogram of the acoustic record showing the Acoustic CPAs of the vessels (B) and the characteristic Lloyds mirror pattern. D) is a distant pass characteristic of a larger vessel. Spectrogram has a frequency resolution of 2 Hz, a frame length of 0.125s, a timestep of 0.03125s, and Hamming window. Colour indicates relative intensity. The 25th and 99.99th percentile amplitude bounds are 61 and 115 dB re 1µPa/Hz respectively.

Figures 16 through 19 present the spectrograms of the acoustic signature of the fishing activity performed by the *Rozafa 11* as part of this trial, recorded at both stations. These activities include the deployment of trawl equipment (A), performing a transit with the net deployed (B), and the final retrieval of the fishing equipment (C). Note that while there are tonals present in the fishing portion of the acoustic record, they do not show the distinctive Lloyds mirror pattern until the end as the vessel was moving around the receivers at a consistent range of approximately 1 km, before approaching the receiver. Moving forward, only fishing activity from station 1 will be considered as the vessel was too far from station 2.

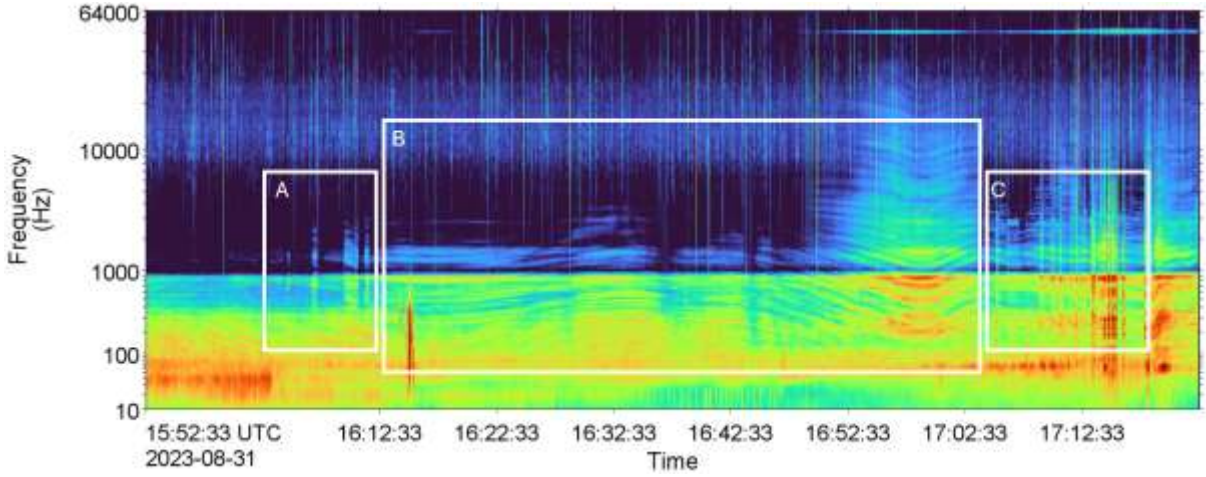

Figure 16. Fishing activity sound analysis of the *Rozafa 11* at Station 1, full band. A) Deployment of the fishing Equipment. B) Performing a trawl. C) Retrieval of the fishing equipment. Spectrogram has a frequency resolution of 2 Hz, a frame length of 0.125s, a timestep of 0.03125s, and Hamming window. Colour indicates relative intensity. The 25th and 99.99th percentile amplitude bounds are 61 and 118dB re 1µPa/Hz respectively.

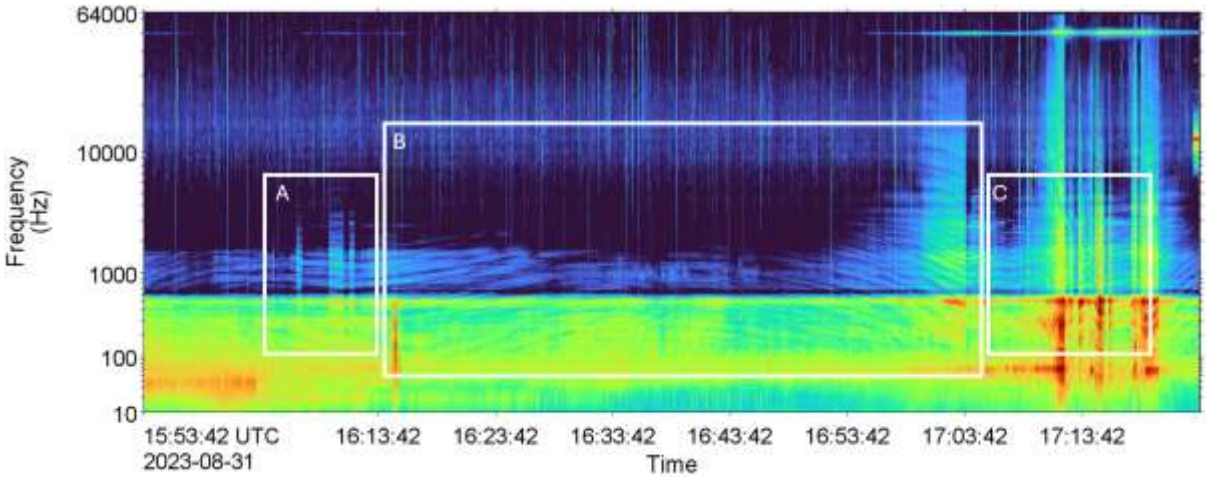

Figure 17. Fishing activity sound analysis of the *Rozafa 11* at Station 2, full band. A) Deployment of the fishing Equipment. B) Performing a trawl. C) Retrieval of the fishing equipment. Spectrogram has a frequency resolution of 2 Hz, a frame length of 0.125s, a timestep of 0.03125s, and Hamming window. Colour indicates relative intensity. The 25th and 99.99th percentile amplitude bounds are 61 and 115dB re 1µPa/Hz respectively.

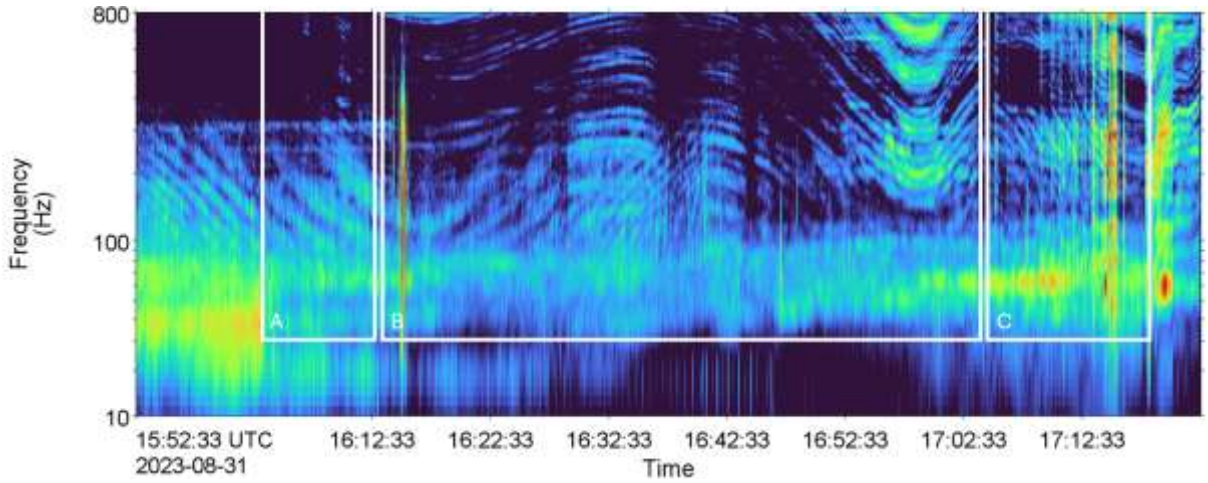

Figure 18 Fishing activity sound analysis of the *Rozafa 11* at Station 1, truncated band. A) Deployment of the fishing Equipment. B) Performing a trawl. C) Retrieval of the fishing equipment. Spectrogram has a frequency resolution of 2 Hz, a frame length of 0.125s, a timestep of 0.03125s, and Hamming window. Colour indicates relative intensity. The 25th and 99.99th percentile amplitude bounds are 61 and 118dB re 1µPa/Hz respectively.

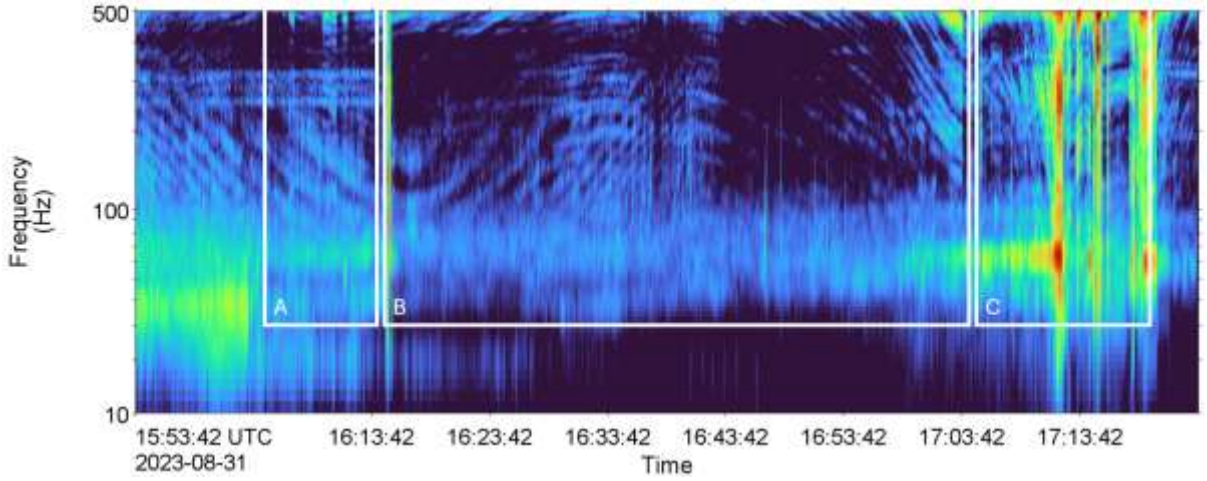

Figure 19 Fishing activity sound analysis of the *Rozafa 11* at Station 2, truncated band. A) Deployment of the fishing Equipment. B) Performing a trawl. C) Retrieval of the fishing equipment. Spectrogram has a frequency resolution of 2 Hz, a frame length of 0.125s, a timestep of 0.03125s, and Hamming window. Colour indicates relative intensity. The 25th and 99.99th percentile amplitude bounds are 61 and 115dB re 1µPa/Hz respectively.

3.2.2. Source Level Estimation

The frequency dependent source levels of *Rozafa 11* in transit, trawling, and retrieval activities were estimated using the method detailed in section 2.4.1. Figure 20 shows the estimated source level as a function of horizontal range for the various trial activities. Band source levels for the vessel transit are obtained from each of the 4 CPA events visible in Figures 12 and 13. Elevated levels of low frequency noise, and the general trend of increasing levels as a function of range, are due to back propagation of ambient noise in the region and are an artifact of this method. The vertical dashed line in each plot represents the approximate range threshold, based on the +-30° azimuth window, where this effect is minimized and inversion for SL is reliable. Bands where the *Rozafa 11* is the dominant source show stable levels with range, such as the 315-1000 Hz band at Station 1, Pass 2.

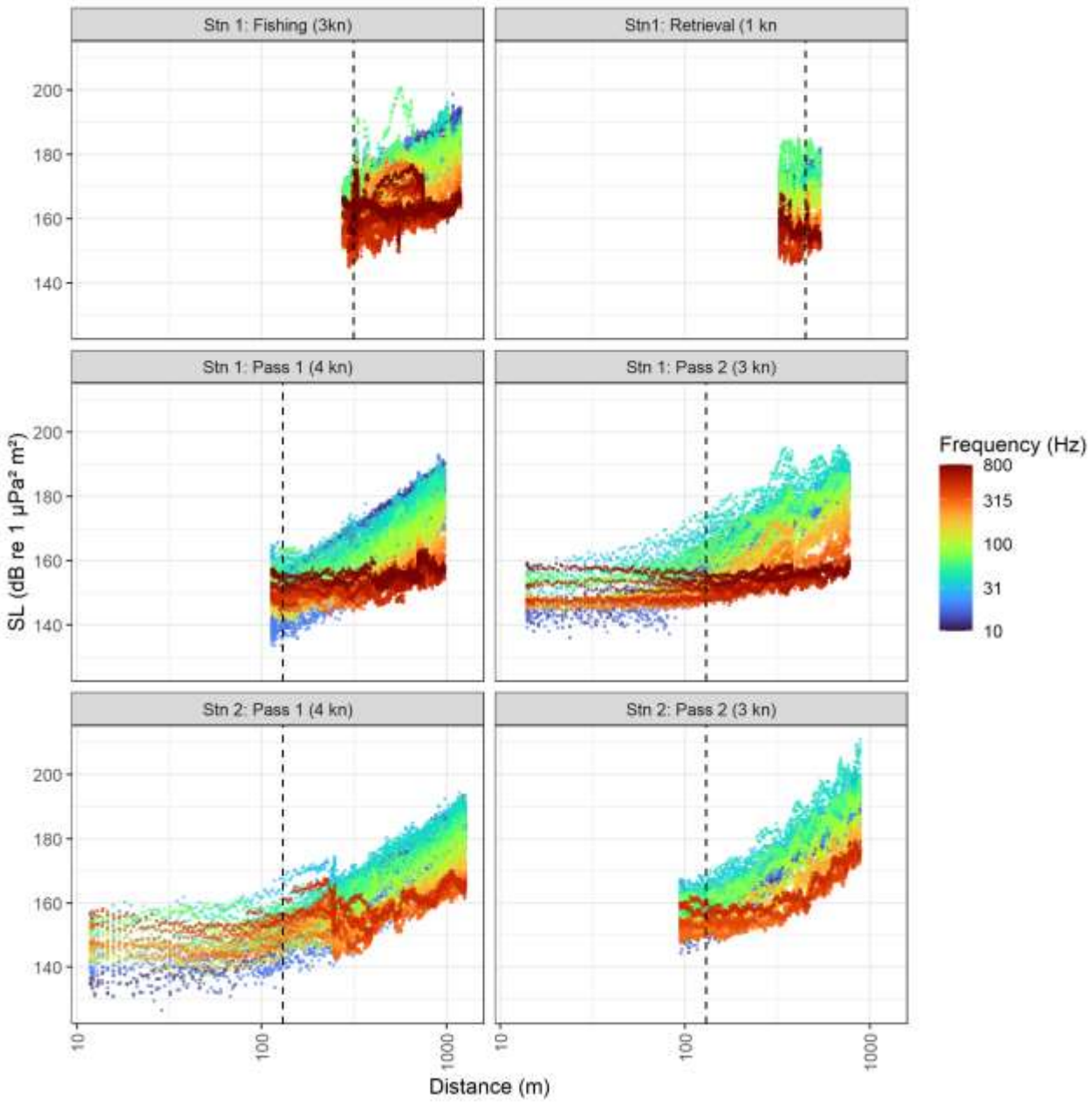

Figure 20. Frequency dependent source level as a function of range for different vessel activities. Top panels: fishing and retrieval activities; Middle panels: vessel transit passes on Station 1; Bottom panels: vessel transit passes on Station 2. Dashed line represents approximate range threshold based on the +-30° azimuth window for SL inversion.

Within the range thresholds, the source levels remain consistent with distance and can be averaged to provide a representative decidecade SL spectrum for each of the three activities (Figure 21, Table 10). For the transit activity, the SLs over the four passes were averaged. Only SL bands up to 800 Hz are reported, as recorded levels at 1kHz and beyond are affected by the air bubbles induced interference and are therefore inaccurate.

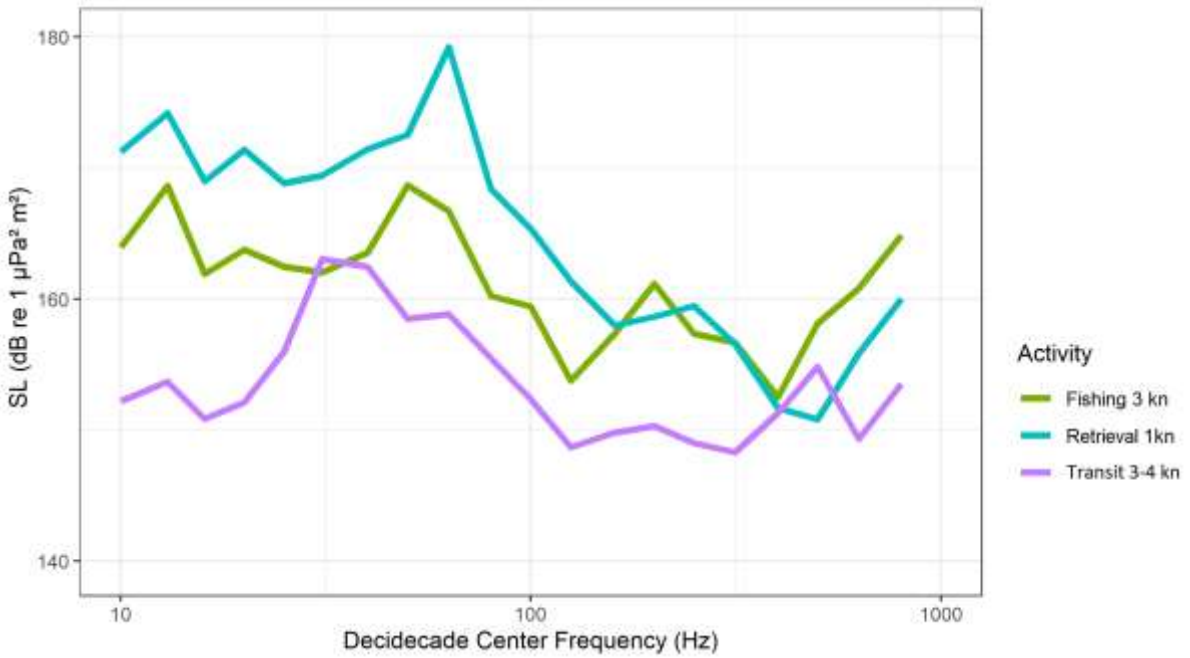

Figure 21. Average source level spectra for the *Rozafa 11* computed using values within the idealized measurement window.

Table 10. Decidecade and broadband source level for the *Rozafa 11* during different activities. Data are truncated at 800 Hz due to bubble effects.

	Source Level (dB re 1 µPa²m²)			
Decidecade Center (Hz)	Transit (3-4 kn)	Fishing (3 kn)	Retrieval (1 kn)	Reference (3.5 kn)
10	152.2	163.9	171.2	120.4
13	153.7	168.7	174.2	121.6
16	150.9	161.9	169.0	122.5
20	152.1	163.8	171.4	123.5
25	156.0	162.5	168.8	124.5
31	163.0	162.0	169.4	125.5
40	162.5	163.5	171.4	126.7
50	158.5	168.7	172.6	127.7
63	158.8	166.7	179.2	128.8
80	155.5	160.2	168.4	129.8
100	152.4	159.4	165.4	130.7
125	148.7	153.8	161.4	131.5
160	149.8	157.4	158.0	132.2
200	150.3	161.2	158.7	132.6
250	149.0	157.4	159.5	132.7
315	148.3	156.7	156.6	132.5
400	151.3	152.5	151.7	131.9
500	154.8	158.1	150.8	131.2
630	152.1	160.8	155.9	130.3
800	156.4	164.9	160.0	129.2
Broadband	169.2	176.2	183.2	142.7

3.3. Ranges to Acoustic Thresholds

3.3.1. Validation of SSC Updated Source Level for OTB-M

This section presents results of sound propagation modelling for the vessel whose SL was obtained from the SSC measurements, in bottom trawl fishing regime. Estimates are shown both of levels near the seafloor at specified ranges (for relevance to benthic species) and of maximum-over-depth threshold ranges, meaning that a specified threshold is reached at that range at some depth in the water column (see Appendix D.1). Corresponding results from the 2021 modelling study, for a bottom trawler category matching the vessel measured in the SSC, are also shown for comparison.

In Figure 22 the decidecade band source level spectrum modelled for the proxy vessel in the 2021 study is superimposed with the SSC-based source level spectrum for the measured vessel in 2023, which is limited to bands below 1 kHz. To assess the relevance of the higher bands to the results, forward modelling is performed both for the truncated source spectrum and for an augmented one in which the modelled band levels from 2021 are used for frequencies above 800 Hz.

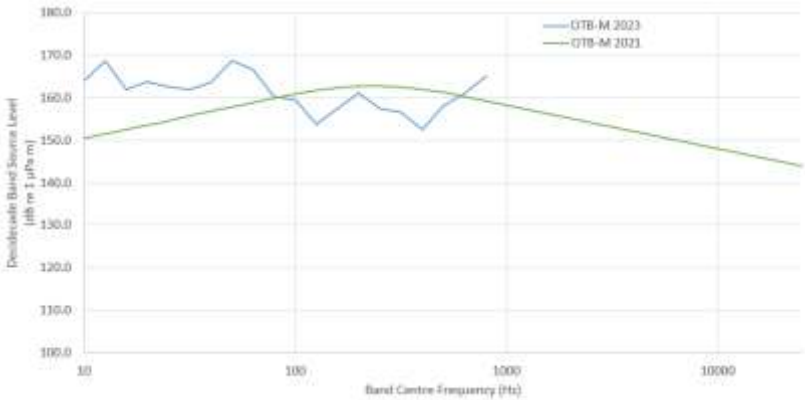

Figure 22. Modelled decidecade band source levels for OTB-M vessel class from the 2021 study, and measurement-based source levels from the 2023 SSC.

Received SPLs near the seabed at 750, 1500, and 3000 m from the source at the six modelled locations are presented in Table 11 for the 10-800 Hz truncated SL spectrum from the 2023 SSC, the same spectrum augmented above 800 Hz with the OTB-M SL band values from 2021, and the original OTB-M SL band values. Results represent the maximum level modelled along any radial around the source at the specified distance, and hence may not be along the same radial for different distances.

Table 11. Modelled SPL near the seabed at three ranges (750, 1500, and 3000 m) from the six modelled locations, for three SL spectra. Levels are the maximum along any radial around the source.

Vessel Type	Distance from source (m)	SPL (dB re 1 µPa) near the seabed					
		Site					
		B1	B2	B3	C1	C2	C3
2023 SSC 10-800 Hz	750	117.3	118.8	117.3	119.3	118.5	116.9
	1500	106.9	108.9	104.1	107.2	109.1	102.2
	3000	95.4	106.6	94.9	105.9	106.8	96.6
2023 SSC augmented	750	117.9	120.4	118.1	120.9	120.2	118
	1500	109.3	109.9	107.1	108.1	110.0	105.1
	3000	95.9	107.7	95.4	107.2	108.1	96.9
2021 modelled OTB-M	750	118.1	120.0	117.9	120.4	119.8	117.7
	1500	108.7	109.6	106.6	108.0	109.6	104.8
	3000	94.4	107.1	93.8	106.9	107.4	93.6

Ranges to various SPL isopleths from each of the six vessel types are listed in Tables 12 to 14. The tabulated results present the maximum and 95% distances (see Appendix D.2).

Table 12. Maximum (R_{max}) and 95% ($R_{95\%}$) horizontal distances (in km) to modelled maximum-over-depth SPL isopleths for the 10-800 Hz SL bands from the 2023 SSC.

SPL (dB re 1 µPa)	B1		B2		B3		C1		C2		C3	
	R_{max}	$R_{95\%}$	R_{max}	$R_{95\%}$	R_{max}	$R_{95\%}$	R_{max}	$R_{95\%}$	R_{max}	$R_{95\%}$	R_{max}	$R_{95\%}$
80	15.3	13.0	56.1	42.8	14.6	11.3	45.6	27.1	38.3	27.1	15.5	13.7
90	4.96	4.65	33.7	19.7	4.85	4.53	22.4	14.2	19.0	14.2	5.14	4.38
100	2.37	2.15	9.71	6.91	2.14	2.02	7.83	6.14	7.13	6.14	2.17	2.08
110	1.33	1.28	2.04	1.89	1.23	1.19	2.04	1.85	1.98	1.85	1.2	1.14
120†	**0.47**	**0.46**	**0.7**	**0.68**	**0.47**	**0.46**	**0.71**	**0.67**	**0.69**	**0.67**	**0.5**	**0.48**
130	0.14	0.14	0.14	0.14	0.14	0.14	0.15	0.14	0.14	0.14	0.14	0.14
140	0.05	0.05	0.05	0.05	0.05	0.05	0.05	0.05	0.05	0.05	0.05	0.05
150	-	-	-	-	-	-	-	-	-	-	-	-

† Behavioural response threshold for marine mammals (NOAA 2019)
A dash indicates the stated level was not reached within the minimum horizontal range step of the modelling.

Table 13. Maximum (R_{max}) and 95% ($R_{95\%}$) horizontal distances (in km) to modelled maximum-over-depth SPL isopleths for the 10-800 Hz SL bands from the 2023 SSC augmented above 800 Hz with the OTB-M SL band values from 2021.

SPL (dB re 1 µPa)	B1		B2		B3		C1		C2		C3	
	R_{max}	$R_{95\%}$	R_{max}	$R_{95\%}$	R_{max}	$R_{95\%}$	R_{max}	$R_{95\%}$	R_{max}	$R_{95\%}$	R_{max}	$R_{95\%}$
80	15.3	13.0	56.1	45.1	14.6	11.3	46.2	29.7	39.4	29.7	15.5	13.7
90	5.34	4.81	33.7	21.7	4.9	4.58	24.1	15.9	20.1	15.9	5.14	4.62
100	2.45	2.21	10.8	7.88	2.22	2.14	10.1	7.02	8.71	7.02	2.18	2.1
110	1.46	1.41	2.46	2.22	1.36	1.32	2.39	2.19	2.43	2.19	1.31	1.26
120†	**0.52**	**0.51**	**0.77**	**0.74**	**0.52**	**0.51**	**0.79**	**0.74**	**0.76**	**0.74**	**0.56**	**0.54**
130	0.16	0.15	0.16	0.16	0.16	0.15	0.16	0.16	0.16	0.16	0.16	0.15
140	0.05	0.05	0.05	0.05	0.05	0.05	0.05	0.05	0.05	0.05	0.05	0.05
150	-	-	-	-	-	-	-	-	-	-	-	-

† Behavioural response threshold for marine mammals (NOAA 2019)
A dash indicates the stated level was not reached within the minimum horizontal range step of the modelling.

Table 14. Maximum (R_{max}) and 95% ($R_{95\%}$) horizontal distances (in km) to modelled maximum-over-depth SPL isopleths for the OTB-M SL band values from 2021.

SPL (dB re 1 µPa)	B1		B2		B3		C1		C2		C3	
	R_{max}	$R_{95\%}$	R_{max}	$R_{95\%}$	R_{max}	$R_{95\%}$	R_{max}	$R_{95\%}$	R_{max}	$R_{95\%}$	R_{max}	$R_{95\%}$
80	8.90	7.74	50.8	42.5	8.03	7.07	45.1	36.0	35.7	27.9	7.78	6.86
90	4.65	4.10	26.6	19.6	4.15	3.91	21.1	17.1	18.8	14.6	4.00	3.75
100	2.43	2.12	8.80	7.36	2.16	2.05	8.01	7.21	7.43	6.67	2.13	2.00
110	1.42	1.37	2.20	2.04	1.32	1.28	2.27	2.07	2.20	2.07	1.27	1.22
120†	**0.61**	**0.60**	**0.74**	**0.72**	**0.60**	**0.59**	**0.77**	**0.74**	**0.74**	**0.72**	**0.60**	**0.58**
130	0.17	0.17	0.19	0.18	0.18	0.17	0.18	0.18	0.18	0.17	0.18	0.17
140	0.05	0.05	0.05	0.05	0.05	0.05	0.05	0.05	0.05	0.05	0.05	0.05
150	–	–	–	–	–	–	–	–	–	–	–	–

† Behavioural response threshold for marine mammals (NOAA 2019)
A dash indicates the stated level was not reached within the minimum horizontal range step of the modelling.

3.3.2. Single Vessel with SSC Updated OTC Source Levels

The source level spectra for the two OTB categories not directly measured in the SSC study were estimated as described in section 2.4.3, by assuming self-similarity of the spectral profiles and offsetting the OTB-M levels by the difference in the modelled broadband SL between categories. The LLS source level spectra, on the other hand, were left unchanged at their original modelled values. The resulting broadband source levels and spectra are presented in Table 15 and Figure 23 respectively for all vessel types. Full decidecade source levels can be found in Appendix E.1.

Table 15. Modelled (LLS) and measurement-adjusted (OTB) broadband monopole source levels for the various vessel categories.

Vessel category		Broadband MSL (dB re 1 µPa·m)
LLS	S	149.2
	M	151.4
	L	152.6
OTB	S	174.4
	M	176.5
	L	178.3

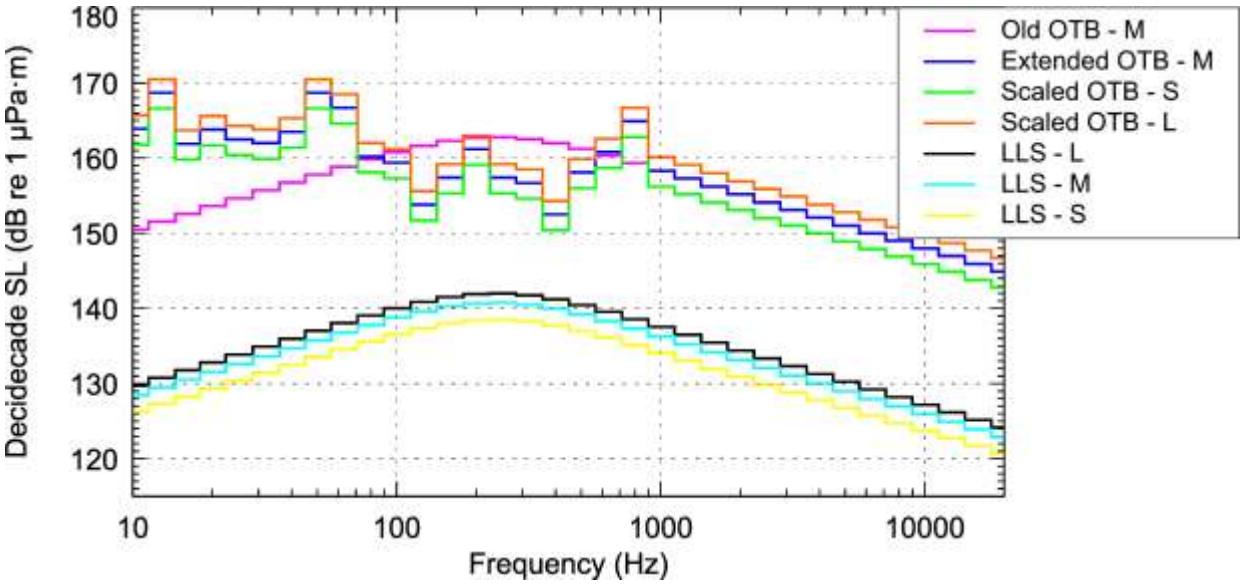

Figure 23. Modelled (LLS) and measurement-adjusted (OTB) source spectra for the three sizes of fishing vessels of each type.

Using these source levels, updated sound propagation results were computed for the three OTB vessel categories. Corresponding results for the three LLS categories, where included for context, are unchanged from the 2021 modelling study.

Received SPLs near the seabed at 750, 1500, and 3000 m from the source are presented in Table 16 for the six vessel categories at the six modelled locations. Ranges to various SPL isopleths from each of the three OTB categories are listed in Tables 17 to 19 (values for the LLS categories, unchanged from the 2021 study and considerably smaller than for the OTB types, are not shown), and , and ranges to the SPL thresholds for fish from Popper et al. (2014) are presented in Table 20.

Table 16. Modelled SPL at three distances (750, 1500, and 3000 m) from each modelled source at all modelled locations. Levels are given near the seabed and are the maximum along any radial around the source.

Vessel Type	Distance from source (m)	SPL (dB re 1 µPa) near the seabed					
		Site					
		B1	B2	B3	C1	C2	C3
LLS – S	750	92.9	94.0	92.5	94.4	93.7	92.1
	1500	82.6	83.9	80.6	82.5	83.9	78.6
	3000	68.3	80.9	67.4	80.7	81.2	67.1
LLS – M	750	96.0	97.7	95.7	98.1	97.5	95.5
	1500	86.4	87.3	84.3	85.8	87.4	82.5
	3000	72.1	84.8	71.4	84.6	85.1	71.3
LLS – L	750	97.6	99.7	97.3	100.0	99.4	97.2
	1500	88.4	89.1	86.3	87.5	89.2	84.6
	3000	74.1	86.8	73.6	86.6	87.0	73.5
Scaled OTB – S	750	115.4	116.6	115.1	117.1	116.4	114.8
	1500	105.3	106.7	103.1	105.2	106.8	101.1
	3000	91.8	103.8	91.2	103.4	104.2	92.2
Augmented OTB – M	750	117.9	120.4	118.1	120.9	120.2	118.0
	1500	109.3	109.9	107.1	108.1	110.0	105.1
	3000	95.9	107.7	95.4	107.2	108.1	96.9
Scaled OTB – L	750	119.3	123.3	119.8	123.6	123.1	120.0
	1500	112.6	112.1	110.3	110.1	112.0	108.4
	3000	99.0	110.6	99.0	110.1	110.9	100.6

Table 17. Maximum (R_{max}) and 95% ($R_{95\%}$) horizontal distances (in km) from the small OTB vessel to modelled maximum-over-depth SPL isopleths.

SPL (dB re 1 µPa)	B1		B2		B3		C1		C2		C3	
	R_{max}	$R_{95\%}$	R_{max}	$R_{95\%}$	R_{max}	$R_{95\%}$	R_{max}	$R_{95\%}$	R_{max}	$R_{95\%}$	R_{max}	$R_{95\%}$
80	9.27	7.52	45.10	35.32	7.72	7.25	38.74	22.55	27.96	22.55	7.89	7.29
90	3.82	3.51	20.16	14.48	3.62	3.18	16.85	11.62	15.33	11.62	3.53	3.38
100	1.97	1.80	6.31	5.02	1.85	1.79	5.26	4.60	5.63	4.60	1.80	1.74
110	1.16	1.11	1.72	1.59	1.09	1.05	1.71	1.57	1.69	1.57	1.05	1.01
120†	**0.39**	**0.38**	**0.56**	**0.54**	**0.39**	**0.38**	**0.54**	**0.54**	**0.55**	**0.54**	**0.41**	**0.39**
130	0.12	0.12	0.12	0.12	0.12	0.12	0.12	0.12	0.12	0.12	0.12	0.12
140	0.03	0.03	0.03	0.03	0.03	0.03	0.03	0.03	0.03	0.03	0.03	0.03
150	-	-	-	-	-	-	-	-	-	-	-	-

† Behavioural response threshold for marine mammals (NOAA 2019)
A dash indicates the stated level was not reached within the minimum horizontal range step of the modelling

Table 18. Maximum (R_{max}) and 95% ($R_{95\%}$) horizontal distances (in km) from the medium OTB vessel to modelled maximum-over-depth SPL isopleths.

SPL (dB re 1 µPa)	B1		B2		B3		C1		C2		C3	
	R_{max}	$R_{95\%}$	R_{max}	$R_{95\%}$	R_{max}	$R_{95\%}$	R_{max}	$R_{95\%}$	R_{max}	$R_{95\%}$	R_{max}	$R_{95\%}$
80	15.31	12.96	56.12	45.05	14.6	11.31	46.17	29.70	39.37	29.70	15.51	13.65
90	5.34	4.81	33.71	21.73	4.90	4.58	24.11	15.89	20.07	15.89	5.14	4.62
100	2.45	2.21	10.80	7.88	2.22	2.14	10.08	7.02	8.71	7.02	2.18	2.10
110	1.46	1.41	2.46	2.22	1.36	1.32	2.39	2.19	2.43	2.19	1.31	1.26
120†	**0.52**	**0.51**	**0.77**	**0.74**	**0.52**	**0.51**	**0.79**	**0.74**	**0.76**	**0.74**	**0.56**	**0.54**
130	0.16	0.15	0.16	0.16	0.16	0.15	0.16	0.16	0.16	0.16	0.16	0.15
140	0.05	0.05	0.05	0.05	0.05	0.05	0.05	0.05	0.05	0.05	0.05	0.05
150	-	-	-	-	-	-	-	-	-	-	-	-

† Behavioural response threshold for marine mammals (NOAA 2019)
A dash indicates the stated level was not reached within the minimum horizontal range step of the modelling

Table 19. Maximum (R_{max}) and 95% ($R_{95\%}$) horizontal distances (in km) from the large OTB vessel to modelled maximum-over-depth SPL isopleths.

SPL (dB re 1 µPa)	B1		B2		B3		C1		C2		C3	
	R_{max}	$R_{95\%}$	R_{max}	$R_{95\%}$	R_{max}	$R_{95\%}$	R_{max}	$R_{95\%}$	R_{max}	$R_{95\%}$	R_{max}	$R_{95\%}$
80	19.29	17.04	71.18	52.92	18.08	16	50.23	36.95	50.83	36.95	19.36	16.63
90	7.42	6.88	40.49	29.36	7.35	6.63	33.17	19.64	24.77	19.64	7.33	6.45
100	3.41	3.01	15.64	10.83	2.99	2.75	13.60	9.53	11.95	9.53	3.07	2.93
110	1.64	1.57	4.43	3.55	1.51	1.46	3.70	3.30	3.72	3.30	1.44	1.38
120†	**0.67**	**0.65**	**0.92**	**0.88**	**0.71**	**0.67**	**0.94**	**0.86**	**0.89**	**0.86**	**0.75**	**0.72**
130	0.20	0.19	0.21	0.21	0.20	0.20	0.21	0.21	0.21	0.21	0.20	0.20
140	0.06	0.06	0.06	0.06	0.06	0.06	0.06	0.06	0.06	0.06	0.06	0.06
150	-	-	-	-	-	-	-	-	-	-	-	-

† Behavioural response threshold for marine mammals (NOAA 2019)
A dash indicates the stated level was not reached within the minimum horizontal range step of the modelling

Table 20. Modelled distances to impact thresholds for fish specified in Popper et al. (2014) from each modelled source at all modelled locations.

Vessel Type	Criteria for Fish: Swim Bladder Involved in Hearing		R_{max} (km)					
			Site					
	Impairment	SPL threshold (dB re 1 µPa)	B1	B2	B3	C1	C2	C3
LLS – S	TTS	158	–	–	–	–	–	–
	Recoverable injury	170	–	–	–	–	–	–
LLS – M	TTS	158	–	–	–	–	–	–
	Recoverable injury	170	–	–	–	–	–	–
LLS – L	TTS	158	–	–	–	–	–	–
	Recoverable injury	170	–	–	–	–	–	–
Scaled OTB – S	TTS	158	<0.02	<0.02	<0.02	<0.02	<0.02	<0.02
	Recoverable injury	170	<0.02	<0.02	<0.02	<0.02	<0.02	<0.02
Augmented OTB – M	TTS	158	<0.02	<0.02	<0.02	<0.02	<0.02	<0.02
	Recoverable injury	170	<0.02	<0.02	<0.02	<0.02	<0.02	<0.02
Scaled OTB – L	TTS	158	<0.02	<0.02	<0.02	<0.02	<0.02	<0.02
	Recoverable injury	170	<0.02	<0.02	<0.02	<0.02	<0.02	<0.02

A dash indicates the level was not reached at any distance from the source

3.3.3. Multiple Vessels with SSC Updated OTC Source Levels

The propagated sound field was modelled as described in Section 2.4.3 for the assumed vessel types and positions (Table 9 and Appendix E.2) for the two scenarios postulated. Results are presented in this section for multiple vessel Scenario 1 (a day where only OTB vessels are allowed to fish in Zone C) and Scenario 2 (a day where only LLS vessels are allowed to fish in Zone C); results are shown in Figures 24 and 25. In Figure 24 it appears as if the modelled sound field passes through some island land masses whereas this in reality would not happen; this a limitation of the methodology of transposing to a new source point a sound field modelled at a different location, but is of minor consequence here.

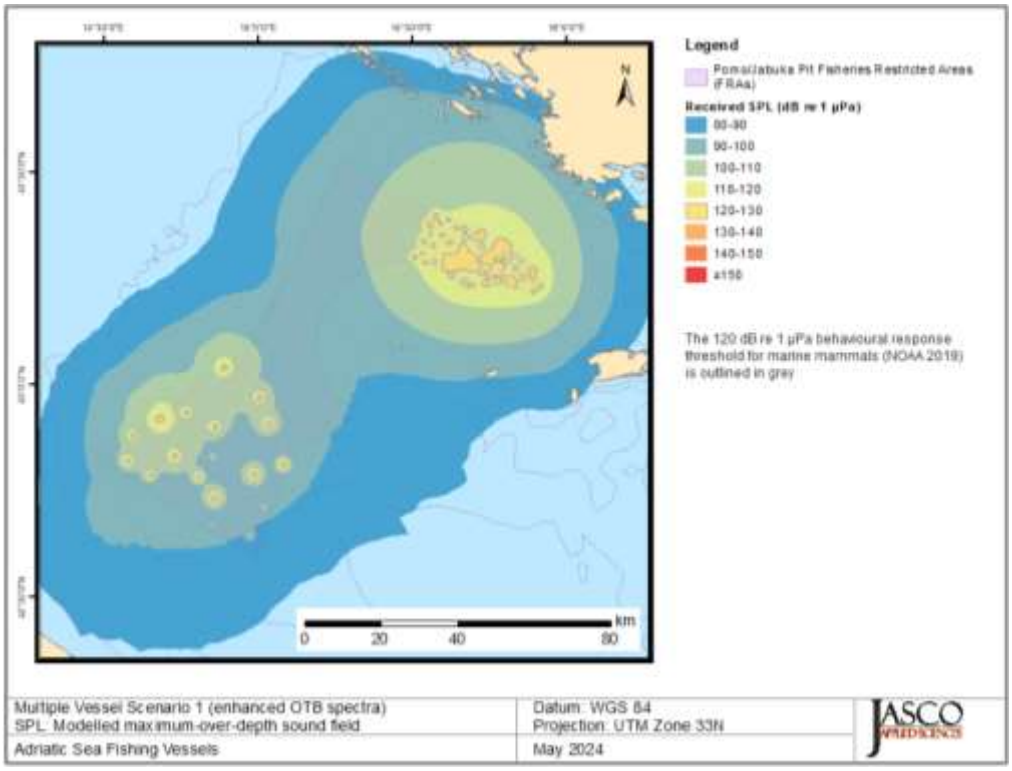

Figure 24. Scenario 1, SPL: Sound level contour map showing unweighted maximum-over-depth results. Modelled vessels are Croatian OTB vessels operating in Zone C and a mixture of Italian LLS and OTB vessels in Zone B representing Saturday-Sunday.

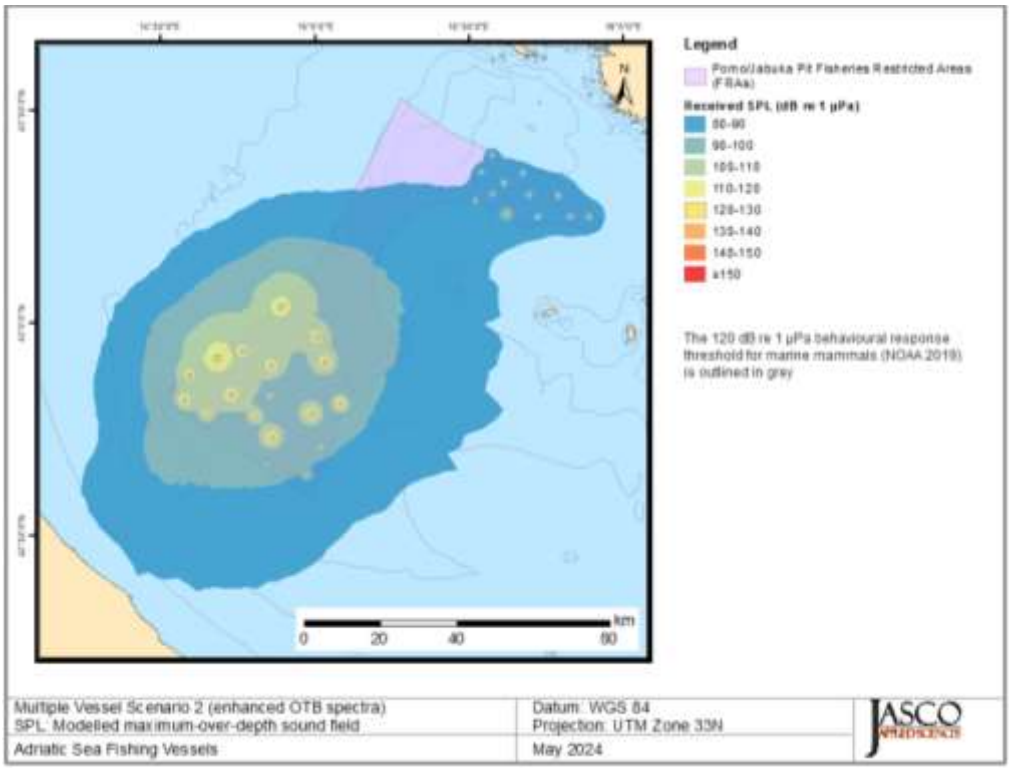

Figure 25. Scenario 2, SPL: Sound level contour map showing unweighted maximum-over-depth results.Modelled vessels are Croatian LLS vessels operating in Zone C and a mixture of Italian LLS and OTB vessels in Zone B representing Monday-Thursday.

4. Discussion and Conclusions

The field study did achieve the intended purpose of collecting acoustic data suitable for determining the underwater acoustic source level of a fishing vessel engaged in bottom trawling activity, yielding reliable band levels over the frequency range of most significant sound emission. An unexpected anomaly did however arise from the design of the hydrophone acoustic casing intended to reduce pseudo-noise from water flow, which substantially degraded the recording of frequencies higher than about 800 Hz and resulted in the limitation of the usable source spectral range obtained from the study. No practicable way could be devised to correct the anomaly in the acoustic data, but within the usable frequency bounds, the identification of relevant vessel signal features in the recordings and the ensuing estimation reliability of the source levels were satisfactory.

4.1. Source Level Estimation from Measurements

The broadband source levels obtained for the fishing trawler *Rozafa 11* that was the object of the SSC appear in line with the few published values from other measurements that were used in the 2021 modelling study as a reference in fine tuning the input parameters for the JOMOPANS-ECHO source level model (MacGillivray and de Jong, (2021). The computed broadband SL of 176 dB re 1 μPa^2m^2 for the *Rozafa 11* in bottom trawling regime (albeit band limited to <1 kHz) compares well, considering the larger size of the subject vessel, with the 173 dB re 1 μPa^2m^2 reported by Daly and White (2021) for a ~20 m long trawler. The spectral shape of the SSC-derived SL in decidecade bands exceeds the trend of the modelled SL for a comparably sized trawler type at frequencies below 100 Hz but lies below it between 100 and about 600 Hz (Figure 22), showing that although the two have similar broadband level the acoustic energy is differently distributed in frequency. It could therefore be expected that the received levels from the two sources might compare variously at different locations and depths subject to the frequency dependent properties of the medium (water and seafloor).

The forward modelling results (Table 11) from the six source locations in the FRA zones B and C confirm the above assessment: even using the 10-800 Hz truncated SL spectrum and thus missing any source energy at and above 1 kHz, the received levels near the seafloor at 750, 1500 and 3000 m range, maximised over all directions, are mostly within 1 dB of those computed from the 2021 modelled SL, with the largest discrepancies being within ~4 dB with no evident sign bias. To further test the relevance of the higher bands to the propagation results in the target acoustic environment of the Pomo/Jabuka Pit FRA, forward modelling was also performed using an augmented SL spectrum in which the modelled band levels from 2021 are used to “fill in” frequencies above 800 Hz. While lacking from the standpoint of providing a fully measurement-based SL, free from source modelling assumptions, this approach enables to carry out full-spectrum modelling of received levels with a source descriptor that is at least as good as the model-based paradigm and strengthened by empirical data in the frequency range containing much of the radiated acoustic energy from the vessel.

4.2. Ranges to Acoustic Thresholds

For the OTB-M vessel type, the modelled $R_{95\%}$ ranges from the six source locations in the FRA to biologically significant sound pressure levels were compared for the fully data-backed truncated SL spectrum (Table 12) and the model-augmented SL spectrum (Table 13). Taking as test levels a) the 120 dB re 1 µPa SPL threshold from NMFS for generic behavioural disturbance of marine mammals and b) the 100 dB re 1 µPa SPL threshold from Borsani and Farchi for behavioural disturbance of LF cetaceans, the comparison shows the range shortfall to be no more than a) 10% and b) 12% for the truncated vs. augmented SL spectra (clearly the latter always yields greater ranges than the former).

The SL characterisation of the *Rozafa 11* achieved from this field study therefore appears reasonably fit for purpose despite lacking the frequency bands above 800 Hz, except of course for modelling exposure levels at 1 kHz and above to assess effects on species mostly sensitive to mid and high frequency sound.

Making the justifiable assumption of self-similarity among the source level spectra of OTB type vessels when engaged in bottom trawl fishing enables the extension of the SSC results to the two vessel categories OTB-S and OTB-L not directly measured in the field campaign. This provides arguably more realistic estimates of their acoustic signatures than the model-based calculation, though still relying on the latter for broadband level scaling with size. The resulting source levels, ranging from 174 to 178 dB re 1 µPa·m, were about 3 dB higher than the corresponding model-only estimates; this however did not translate uniformly into longer ranges to biologically relevant thresholds compared to the 2021 study because of the different frequency distribution of acoustic energy which influenced the long-range propagation of the sound.

SPL values near the seabed were estimated at three distances (750, 1500, and 3000 m) from the modelled single vessel source locations to assess the impact on the demersal fauna of interest. Focusing on the updated OTB results only, the predicted levels at 750 m ranged from 115 to 124 dB re 1 µPa (at B3 and C1 respectively), levels at 1500 m ranged from 101 to 113 dB re 1 µPa (at C3 and B1 respectively), and levels at 3000 m ranged from 91 to 111 dB re 1 µPa (at B3 and C2 respectively). The SPL thresholds for recoverable injury and TTS in pressure sensitive fishes from Popper et al. (2014) of 170 and 158 dB re 1 µPa respectively were not reached for any vessel at any location within the resolution of the modelling (20 m), though source levels for all sizes of OTB vessels exceeded these values. The ranges to these thresholds for OTB vessels can therefore be considered to lie at some distance within 20 m of the source. Ranges to the behavioural response threshold for marine mammals from NOAA (2019) of 120 dB re 1 µPa varied between 0.38 and 0.94 km for OTB vessels. Ranges to levels below approximately 110 dB re 1 µPa are significantly larger at the shallower sites (B2, C1, and C2) compared to the deeper sites (B1, B3, and C3). This is likely an effect of the interaction of the emitted sound with the sea surface and seabed especially given the difference in geoacoustics: the coarser grained sediment at the shallower sites is more reflective than the softer sediment in the deeper waters and thus conducive to enhanced propagation of sound.

Results of the multiple vessel scenarios indicated that with vessels operating in close proximity there is some coalescing of the individual sound fields into a single larger sound field, which is dominated by the noise from OTB vessels as evidenced by comparing Figures 24 (Scenario 1) and 25 (Scenario 2). In Scenario 1 with only OTB vessels operating in Zone C (representing Saturday-Sunday), the entirety of that Zone is ensonified above 110 dB re 1 µPa and there are some coalesced areas ensonified above 120 dB re 1 µPa where several large and medium OTB vessels are working near each other. By contrast in Scenario 2 with only LLS vessels operating in Zone C (representing Monday-Thursday), the overall ensonification is much lower and the footprints of the smaller, quieter LLS vessels do not coalesce save at levels well below 100 dB re 1 µPa.

Literature Cited

[ANSI] American National Standards Institute and [ASA] Acoustical Society of America. S1.1-2013. *American National Standard: Acoustical Terminology*. NY, USA. https://webstore.ansi.org/Standards/ASA/ANSIASAS12013.

[ISO] International Organization for Standardization. 2017a. *ISO 18405:2017. Underwater acoustics – Terminology*. Geneva. https://www.iso.org/standard/62406.html.

[ISO] International Organization for Standardization. 2017b. *ISO 18406:2017(E). Underwater acoustics – Measurement of radiated underwater sound from percussive pile driving*. Geneva. https://www.iso.org/obp/ui/#iso:std:iso:18406:ed-1:v1:en.

[NRC] National Research Council (US). 2003. *Ocean Noise and Marine Mammals*. National Research Council (US), Ocean Studies Board, Committee on Potential Impacts of Ambient Noise in the Ocean on Marine Mammals. The National Academies Press, Washington, DC, USA. https://doi.org/10.17226/10564.

Ainslie, M.A., J.L. Miksis-Olds, S.B. Martin, K.D. Heaney, C.A.F. de Jong, A.M. von Benda-Beckmann, and A.P. Lyons. 2018. *ADEON Underwater Soundscape and Modeling Metadata Standard*. Version 1.0. Technical report by JASCO Applied Sciences for ADEON Prime Contract No. M16PC00003. 35 p. https://doi.org/10.6084/m9.figshare.6792359.v2.

Ainslie, M.A., S.B. Martin, K.B. Trounce, D.E. Hannay, J.M. Eickmeier, T.J. Deveau, K. Lucke, A.O. MacGillivray, V. Nolet, et al. 2022. International harmonization of procedures for measuring and analyzing of vessel underwater radiated noise. *Marine Pollution Bulletin* 174: 113124. https://doi.org/10.1016/j.marpolbul.2021.113124.

Andrew, R.K., B.M. Howe, and J.A. Mercer. 2011. Long-time trends in ship traffic noise for four sites off the North American West Coast. *Journal of the Acoustical Society of America* 129(2): 642-651. https://doi.org/10.1121/1.3518770.

Bailey, H., G. Clay, E.A. Coates, D. Lusseau, B. Senior, and P.M. Thompson. 2010. Using T-PODs to assess variations in the occurrence of coastal bottlenose dolphins and harbour porpoises. *Aquatic Conservation: Marine and Freshwater Ecosystems* 20(2): 150-158. https://doi.org/10.1002/aqc.1060.

Bom, N. 1969. Effect of rain on underwater noise level. *Journal of the Acoustical Society of America* 45(1): 150-156. https://doi.org/10.1121/1.1911351.

[ANSI] American National Standards Institute and [ASA] Acoustical Society of America. S1.1-2013. *American National Standard: Acoustical Terminology*. NY, USA. https://webstore.ansi.org/Standards/ASA/ANSIASAS12013.

[ISO] International Organization for Standardization. 2017a. *ISO 18405:2017. Underwater acoustics – Terminology*. Geneva. https://www.iso.org/standard/62406.html.

[ISO] International Organization for Standardization. 2017b. *ISO 18406:2017(E). Underwater acoustics – Measurement of radiated underwater sound from percussive pile driving*. Geneva. https://www.iso.org/obp/ui/#iso:std:iso:18406:ed-1:v1:en.

[NOAA] National Oceanic and Atmospheric Administration (US). 2019. *ESA Section 7 Consultation Tools for Marine Mammals on the West Coast* (webpage), 27 Sep 2019. https://www.fisheries.noaa.gov/west-coast/endangered-species-conservation/esa-section-7-consultation-tools-marine-mammals-west.

[NRC] National Research Council (US). 2003. *Ocean Noise and Marine Mammals*. National Research Council (US), Ocean Studies Board, Committee on Potential Impacts of Ambient Noise in the Ocean on Marine Mammals. The National Academies Press, Washington, DC, USA. https://doi.org/10.17226/10564.

Ainslie, M.A., J.L. Miksis-Olds, S.B. Martin, K.D. Heaney, C.A.F. de Jong, A.M. von Benda-Beckmann, and A.P. Lyons. 2018. *ADEON Underwater Soundscape and Modeling Metadata Standard*. Version 1.0. Technical report by JASCO Applied Sciences for ADEON Prime Contract No. M16PC00003. 35 p. https://doi.org/10.6084/m9.figshare.6792359.v2.

Ainslie, M.A., S.B. Martin, K.B. Trounce, D.E. Hannay, J.M. Eickmeier, T.J. Deveau, K. Lucke, A.O. MacGillivray, V. Nolet, et al. 2022. International harmonization of procedures for measuring and analyzing of vessel underwater radiated noise. *Marine Pollution Bulletin* 174: 113124. https://doi.org/10.1016/j.marpolbul.2021.113124.

Andrew, R.K., B.M. Howe, and J.A. Mercer. 2011. Long-time trends in ship traffic noise for four sites off the North American West Coast. *Journal of the Acoustical Society of America* 129(2): 642-651. https://doi.org/10.1121/1.3518770.

Bailey, H., G. Clay, E.A. Coates, D. Lusseau, B. Senior, and P.M. Thompson. 2010. Using T-PODs to assess variations in the occurrence of coastal bottlenose dolphins and harbour porpoises. *Aquatic Conservation: Marine and Freshwater Ecosystems* 20(2): 150-158. https://doi.org/10.1002/aqc.1060.

Bom, N. 1969. Effect of rain on underwater noise level. *Journal of the Acoustical Society of America* 45(1): 150-156. https://doi.org/10.1121/1.1911351.

Collins, M.D. 1993. A split-step Padé solution for the parabolic equation method. *Journal of the Acoustical Society of America* 93(4): 1736-1742. https://doi.org/10.1121/1.406739.
Collins, M.D., R.J. Cederberg, D.B. King, and S. Chin-Bing. 1996. Comparison of algorithms for solving parabolic wave equations. *Journal of the Acoustical Society of America* 100(1): 178-182. https://doi.org/10.1121/1.415921.
Cotter, E., J. McVey, L. Weicht, and J. Haxel. 2024. Performance of three hydrophone flow shields in a tidal channel. *JASA Express Letters* 4(1). https://doi.org/10.1121/10.0024333.
Daly, E. and M. White. 2021. Bottom trawling noise: Are fishing vessels polluting to deeper acoustic habitats? *Marine Pollution Bulletin* 162: 111877. https://doi.org/10.1016/j.marpolbul.2020.111877.
Delarue, J.J.-Y., K.A. Kowarski, E.E. Maxner, J.T. MacDonnell, and S.B. Martin. 2018. *Acoustic Monitoring Along Canada's East Coast: August 2015 to July 2017*. Document Number 01279, Environmental Studies Research Funds Report Number 215, Version 1.0. Technical report by JASCO Applied Sciences for Environmental Studies Research Fund, Dartmouth, NS, Canada. 120 pp + appendices.
Fisher, F.H. and V.P. Simmons. 1977. Sound absorption in sea water. *Journal of the Acoustical Society of America* 62(3): 558-564. https://doi.org/10.1121/1.381574.
Heindsmann, T.E., R.H. Smith, and A.D. Arneson. 1955. Effect of rain upon underwater noise levels [Letter to editor]. *Journal of the Acoustical Society of America* 27(2): 378-379. https://doi.org/10.1121/1.1907897.
Knudsen, V.O., R.S. Alford, and J.W. Emling. 1948. Underwater ambient noise. *Journal of Marine Research* 7: 410-429.
Krause, B. 2008. Anatomy of the Soundscape: Evolving Perspectives. *Journal of the Audio Engineering Society* 56(1/2): 73-80. http://www.aes.org/e-lib/browse.cfm?elib=14377.
MacGillivray, A.O. and C.A.F. de Jong. 2021. A Reference Spectrum Model for Estimating Source Levels of Marine Shipping Based on Automated Identification System Data. *Journal of Marine Science and Engineering* 9(4): 369. https://doi.org/10.3390/jmse9040369.
Martin, S.B., C. Morris, K. Bröker, and C. O'Neill. 2019. Sound exposure level as a metric for analyzing and managing underwater soundscapes. *Journal of the Acoustical Society of America* 146(1): 135-149. https://doi.org/10.1121/1.5113578.
Martin, S.B., B.J. Gaudet, H. Klinck, P.J. Dugan, J.L. Miksis-Olds, D.K. Mellinger, D.A. Mann, O. Boebel, C.C. Wilson, et al. 2021. Hybrid millidecade spectra: A practical format for exchange of long-term ambient sound data. *JASA Express Letters* 1(1). https://doi.org/10.1121/10.0003324.
Miksis-Olds, J.L. and S.M. Nichols. 2016. Is low frequency ocean sound increasing globally? *Journal of the Acoustical Society of America* 139(1): 501-511. https://doi.org/10.1121/1.4938237.
Nieukirk, S.L., K.M. Stafford, D.K. Mellinger, R.P. Dziak, and C.G. Fox. 2004. Low-frequency whale and seismic airgun sounds recorded in the mid-Atlantic Ocean. *Journal of the Acoustical Society of America* 115(4): 1832-1843. https://doi.org/10.1121/1.1675816.
Pace, F., S.J. Welch, N. Ferri, and A. Nastasi. 2023. Footprint of Sound Emissions from Fishing Vessels in the Adriatic Sea. *In* Popper, A.N., J. Sisneros, A.D. Hawkins, and F. Thomsen (eds.). *The Effects of Noise on Aquatic Life: Principles and Practical Considerations*. Springer International Publishing, Cham. pp. 1-28. https://doi.org/10.1007/978-3-031-10417-6_120-1.
Popper, A.N., A.D. Hawkins, R.R. Fay, D.A. Mann, S. Bartol, T.J. Carlson, S. Coombs, W.T. Ellison, R.L. Gentry, et al. 2014. *Sound Exposure Guidelines for Fishes and Sea Turtles: A Technical Report prepared by ANSI-Accredited Standards Committee S3/SC1 and registered with ANSI*. ASA S3/SC1.4 TR-2014. SpringerBriefs in Oceanography. ASA Press and Springer. https://doi.org/10.1007/978-3-319-06659-2.
Porter, M.B. and Y.C. Liu. 1994. Finite-element ray tracing. *In*: Lee, D. and M.H. Schultz (eds.). *International Conference on Theoretical and Computational Acoustics*. Volume 2. World Scientific Publishing Co. pp. 947-956.
Robinson, S.P., P.A. Lepper, and R.A. Hazelwood. 2014. Good Practice Guide for Underwater Noise Measurement. *In* National Measurement Office, Marine Scotland, and The Crown Estate (eds.). *NPL Good Practice Guide No. 133*. National Physical Laboratory. p. 97.
Ross, D. 1976. *Mechanics of Underwater Noise*. Pergamon Press, NY, USA.
Scrimger, J.A., D.J. Evans, G.A. McBean, D.M. Farmer, and B.R. Kerman. 1987. Underwater noise due to rain, hail, and snow. *Journal of the Acoustical Society of America* 81(1): 79-86. https://doi.org/10.1121/1.394936.
Strasberg, M. 1979. Nonacoustic noise interference in measurements of infrasonic ambient noise. *Journal of the Acoustical Society of America* 66(5): 1487-1493. https://doi.org/10.1121/1.383543.
Urick, R.J. 1983. *Principles of Underwater Sound*. 3rd edition. McGraw-Hill, New York, London. 423 p.
Wenz, G.M. 1962. Acoustic Ambient Noise in the Ocean: Spectra and Sources. *Journal of the Acoustical Society of America* 34(12): 1936-1956. https://doi.org/10.1121/1.1909155.
Willis, J. and F.T. Dietz. 1961. Effect of Tidal Currents on 25 cps Shallow Water Ambient Noise Measurements. *Journal of the Acoustical Society of America* 33(11): 1659-1659. https://doi.org/10.1121/1.1936636.
Zhang, Z.Y. and C.T. Tindle. 1995. Improved equivalent fluid approximations for a low shear speed ocean bottom. *Journal of the Acoustical Society of America* 98(6): 3391-3396. https://doi.org/10.1121/1.413789.

Daly, E. and M. White. 2021. Bottom trawling noise: Are fishing vessels polluting to deeper acoustic habitats? *Marine Pollution Bulletin* 162: 111877. https://www.sciencedirect.com/science/article/pii/S0025326X20309954.

Delarue, J.J.-Y., K.A. Kowarski, E.E. Maxner, J.T. MacDonnell, and S.B. Martin. 2018. *Acoustic Monitoring Along Canada's East Coast: August 2015 to July 2017*. Document Number 01279, Environmental Studies Research Funds Report Number 215, Version 1.0. Technical report by JASCO Applied Sciences for Environmental Studies Research Fund, Dartmouth, NS, Canada. 120 pp + appendices.

Heindsmann, T.E., R.H. Smith, and A.D. Arneson. 1955. Effect of rain upon underwater noise levels [Letter to editor]. *Journal of the Acoustical Society of America* 27(2): 378-379. https://doi.org/10.1121/1.1907897.

Knudsen, V.O., R.S. Alford, and J.W. Emling. 1948. Underwater ambient noise. *Journal of Marine Research* 7: 410-429.

Krause, B. 2008. Anatomy of the Soundscape: Evolving Perspectives. *Journal of the Audio Engineering Society* 56(1/2): 73-80. http://www.aes.org/e-lib/browse.cfm?elib=14377.

MacGillivray, A.O. and C.A.F. de Jong. 2021. A Reference Spectrum Model for Estimating Source Levels of Marine Shipping Based on Automated Identification System Data. *Journal of Marine Science and Engineering* 9(4). https://doi.org/10.3390/jmse9040369.

Martin, S.B., C. Morris, K. Bröker, and C. O'Neill. 2019. Sound exposure level as a metric for analyzing and managing underwater soundscapes. *Journal of the Acoustical Society of America* 146(1): 135-149. https://doi.org/10.1121/1.5113578.

Martin, S.B., B.J. Gaudet, H. Klinck, P.J. Dugan, J.L. Miksis-Olds, D.K. Mellinger, D.A. Mann, O. Boebel, C.C. Wilson, et al. 2021. Hybrid millidecade spectra: A practical format for exchange of long-term ambient sound data. *JASA Express Letters* 1(1). https://doi.org/10.1121/10.0003324.

Miksis-Olds, J.L. and S.M. Nichols. 2016. Is low frequency ocean sound increasing globally? *Journal of the Acoustical Society of America* 139(1): 501-511. https://doi.org/10.1121/1.4938237.

Nieukirk, S.L., K.M. Stafford, D.K. Mellinger, R.P. Dziak, and C.G. Fox. 2004. Low-frequency whale and seismic airgun sounds recorded in the mid-Atlantic Ocean. *Journal of the Acoustical Society of America* 115(4): 1832-1843. https://doi.org/10.1121/1.1675816.

Pace, F., S.J. Welch, N. Ferri, and A. Nastasi. 2023. Footprint of Sound Emissions from Fishing Vessels in the Adriatic Sea. *In* Popper, A.N., J. Sisneros, A.D. Hawkins, and F. Thomsen (eds.). *The Effects of Noise on Aquatic Life: Principles and Practical Considerations*. Springer International Publishing, Cham. pp. 1-28. https://doi.org/10.1007/978-3-031-10417-6_120-1.

Plomp, R. and M.A. Bouman. 1959. Relation between Hearing Threshold and Duration for Tone Pulses. *Journal of the Acoustical Society of America* 31(6): 749-758. https://doi.org/10.1121/1.1907781.

Robinson, S.P., P.A. Lepper, and R.A. Hazelwood. 2014. Good Practice Guide for Underwater Noise Measurement. *In* National Measurement Office, Marine Scotland, and The Crown Estate (eds.). *NPL Good Practice Guide No. 133*. National Physical Laboratory. p. 97.

Ross, D. 1976. *Mechanics of Underwater Noise*. Pergamon Press, NY, USA.

Scrimger, J.A., D.J. Evans, G.A. McBean, D.M. Farmer, and B.R. Kerman. 1987. Underwater noise due to rain, hail, and snow. *Journal of the Acoustical Society of America* 81(1): 79-86. https://doi.org/10.1121/1.394936.

Strasberg, M. 1979. Nonacoustic noise interference in measurements of infrasonic ambient noise. *Journal of the Acoustical Society of America* 66(5): 1487-1493. https://doi.org/10.1121/1.383543.

Urick, R.J. 1983. *Principles of Underwater Sound*. 3rd edition. McGraw-Hill, New York, London. 423 p.

Wenz, G.M. 1962. Acoustic Ambient Noise in the Ocean: Spectra and Sources. *Journal of the Acoustical Society of America* 34(12): 1936-1956. https://doi.org/10.1121/1.1909155.

Willis, J. and F.T. Dietz. 1961. Effect of Tidal Currents on 25 cps Shallow Water Ambient Noise Measurements. *Journal of the Acoustical Society of America* 33(11): 1659-1659. https://doi.org/10.1121/1.1936636.

Appendix A. Recorder Calibration

Each AMAR was calibrated before deployment and upon retrieval (battery life permitting) with a pistonphone type 42AC precision sound source (G.R.A.S. Sound & Vibration A/S; Figure A-1). The pistonphone calibrator produces a constant tone at 250 Hz at a fixed distance from the hydrophone sensor in an airtight space of known volume. The recorded level of the reference tone on the AMAR yields the system gain for the AMAR and hydrophone. To determine absolute sound pressure levels, this gain was applied during data analysis. Typical calibration variance using this method is less than 0.7 dB absolute pressure.

Figure A-1.Split view of a G.R.A.S. 42AC pistonphone calibrator with an M36 hydrophone.

Appendix B. Fishing Activity Log

Table B-1. Complete *Rozafa 11* activity log recorded for the duration of the trial

Rozafa 11 Tack notes						GPS SN: 61	12.0m		
						Sea sate	2		
First pass over amar: Normal fishing speed (3kt)						Depth	48 - 56.6m		
Start time	14:55	One way, starting 1				Vessel noise	Generator, engine		
End tme:	15:20	mile away					and deoth sounder		
						Draft	2.8m		
Start time	15:22	One way, starting 1							
End time:	15:54	km away							
Transectr #1 ~800m away from AMARs									
Time		Speed (kt):		Notes:					
	16:04		2		Begin to deploy net				
	16:06		3		initial drop				
	16:07		3.5		fully deployed net				
	16:09		7		Dropped trawl doors				
	16:10		4		ed up speed with everything depl				
	16:11		drift		Cut engine to drift				
	16:11		3		Fishingcruise speed				
	16:27		3		Begin to turn to reverse course				
	16:32		4						
	16:42		3						
Transectr #2 ~500m away from AMARs									
	16:45		3		Turn complete				
	17:02		1		o bring in net / gear - cable being p				
	17:03		2.5		reversed				
	17:05		3		down to 1kt				
	17:06		1		Trwal doors in				
	17:07		1		Net on sea surface				
	17:08		0-1						
	17:10				line in - nbet coming in				
	17:12		1.5-1						
Additional notes									
Time									
	17:08	Rozafa 23 is ~200m away - port bow and closing							
	17:11	Approx right over AMAR 624							
	17:11	Crossing starboard bow							
	17:12	Starboard alongside Rozafa 11							

Appendix C. Acoustic Data Analysis

The sampled data were processed for ambient sound analysis, vessel noise detection, and detection of all marine mammal vocalizations with JASCO's PAMlab acoustic analysis software suite. The major processing stages are outlined in Figure C-1. The results are calclutaed in terms of various acoustics metrics, defined in Appendix C.1, and in various frequency bands, defined in Appendix C.2.

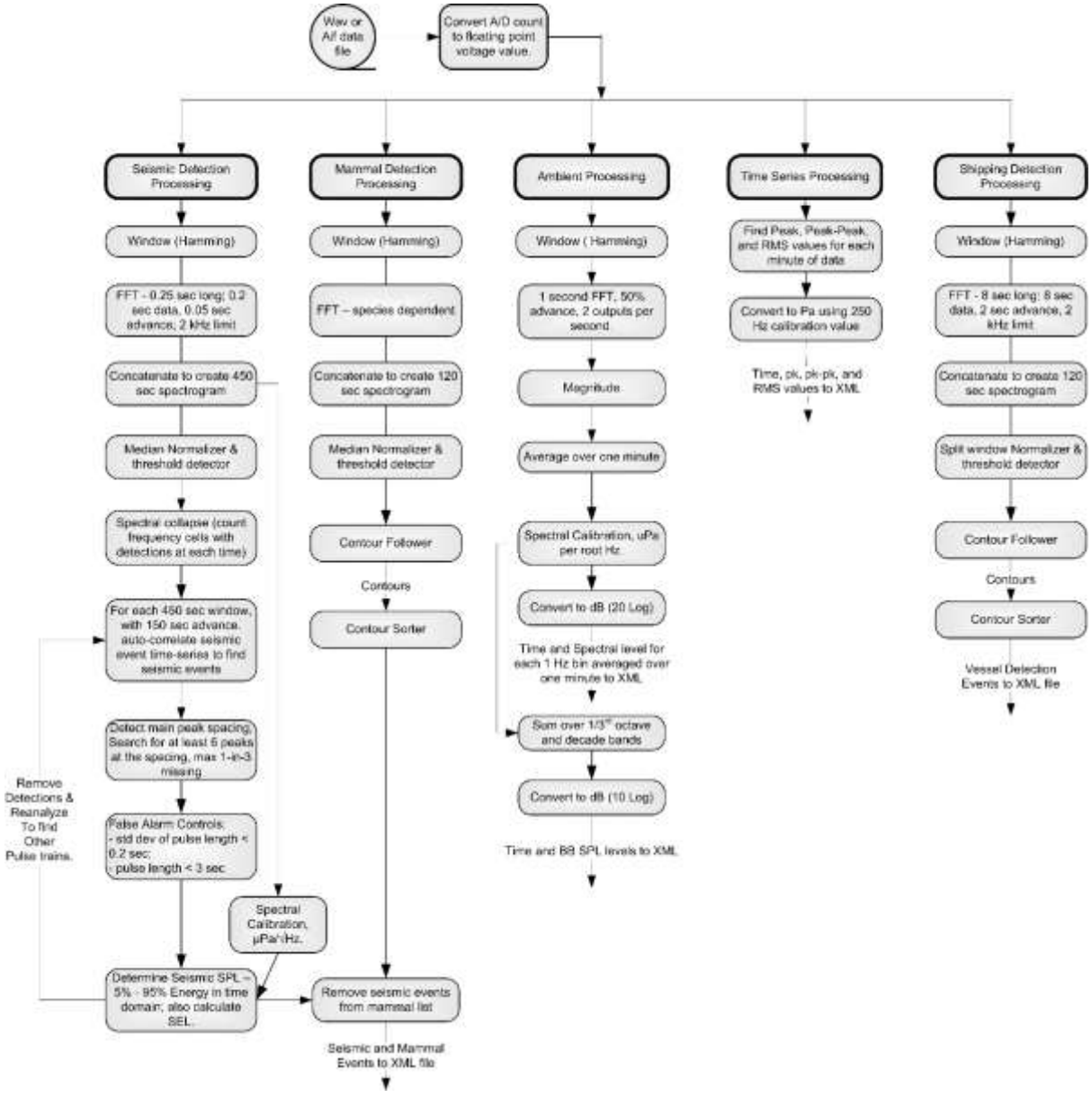

Figure C-1. Major stages of the automated acoustic analysis process performed with JASCO's PAMlab software suite.

C.1. Acoustic Metrics

Underwater sound pressure amplitude is quantified in decibels (dB) relative to a fixed reference pressure of p_0 = 1 µPa. Because the perceived loudness of sound, especially pulsed sound such as from seismic airguns, pile driving, and sonar, is not generally proportional to the instantaneous acoustic pressure, several sound level metrics are commonly used to evaluate sound and its effects

on marine life. Here we provide specific definitions of relevant metrics used in the accompanying report. Where possible, we follow International Organization for Standardization definitions and symbols for sound metrics (e.g., ISO 18405:2017a, ANSI S1.1-2013).

Zero-to-peak sound pressure (PK)

The zero-to-peak sound pressure, or peak sound pressure (PK or L_{pk}; dB re 1 µPa), is the decibel level of the maximum instantaneous sound pressure in a stated frequency band attained by an acoustic pressure signal, $p(t)$:

$$L_{\mathrm{pk}} = 10\log_{10}\frac{p_{\mathrm{pk}}^2}{p_0^2} = 20\log_{10}\frac{p_{\mathrm{pk}}}{p_0} = 20\log_{10}\frac{\max|p(t)|}{p_0}. \quad \text{(C-1)}$$

PK is often included as a criterion for assessing whether a sound is potentially injurious; however, because it does not account for the duration of an acoustic event, it is generally a poor indicator of perceived loudness.

Sound pressure level (SPL)

The sound pressure level (SPL or L_p; dB re 1 µPa) is the root-mean-square (rms) pressure level in a stated frequency band over a specified time window (T; s):

$$L_p = 10\log_{10}\frac{p_{\mathrm{rms}}^2}{p_0^2} = 10\log_{10}\left(\frac{1}{T}\int_T p^2(t)\,dt \Big/ p_0^2\right). \quad \text{(C-2)}$$

It is important to note that SPL always refers to an rms pressure level (i.e., a quadratic mean over a time interval) and therefore not instantaneous pressure at a fixed point in time. The SPL can also be defined as the *mean-square* pressure level, given in decibels relative to a reference value of 1 µPa^2 (i.e., in dB re 1 µPa^2). The two definitions of SPL are numerically equivalent, differing only in reference value.

Energy equivalent SPL (L_{eq})

Energy equivalent SPL (L_{eq}; dB re 1 µPa) denotes the SPL of a stationary (constant amplitude) sound that generates the same SEL as the signal being examined, $p(t)$, over the same time period, T:

$$L_{\mathrm{eq}} = 10\log_{10}\left(\frac{1}{T}\int_T p^2(t)\,dt \Big/ p_0^2\right). \quad \text{(C-3)}$$

The equations for SPL and the energy-equivalent SPL are numerically identical. Conceptually, the difference between the two metrics is that the SPL is typically computed over short periods (typically of 1 s or less) and tracks the fluctuations of a non-steady acoustic signal, whereas the L_{eq} reflects the average SPL of an acoustic signal over time periods typically of 1 min to several hours.

C.2. Decidecade Band Analysis

The distribution of a sound's power with frequency is described by the sound's spectrum. The sound spectrum can be split into a series of adjacent frequency bands. Splitting a spectrum into 1 Hz wide bands, called passbands, yields the power spectral density of the sound. This splitting of the spectrum into passbands of a constant width of 1 Hz, however, does not represent how animals perceive sound.

Animals perceive exponential increases in frequency rather than linear increases, so analyzing a sound spectrum with passbands that increase exponentially in size better approximates real-world scenarios. In underwater acoustics, a spectrum is commonly split into decidecade bands, which are one tenth of a decade wide. A decidecade is sometimes referred to as a "1/3-octave" because one

tenth of a decade is approximately equal to one third of an octave. Each decade represents a factor of 10 in sound frequency. Each octave represents a factor of 2 in sound frequency. The centre frequency of the ith decidecade band, $f_c(i)$, is defined as:

$$f_c(i) = 10^{\frac{i}{10}} \text{ kHz}\,, \tag{C-4}$$

and the low (f_{lo}) and high (f_{hi}) frequency limits of the ith decidecade band are defined as:

$$f_{\text{lo},i} = 10^{\frac{-1}{20}} f_c(i) \text{ and } f_{\text{hi},i} = 10^{\frac{1}{20}} f_c(i)\,. \tag{C-5}$$

The decidecade bands become wider with increasing frequency, and on a logarithmic scale the bands appear equally spaced (Figure C-2).

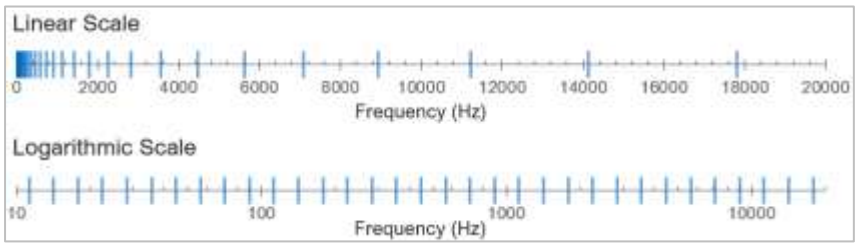

Figure C-2. Decidecade frequency bands (vertical lines) shown on (top) a linear frequency scale and (bottom) a logarithmic scale. On the logarithmic scale, the bands are equally spaced.

The sound pressure level in the ith band ($L_{p,i}$) is computed from the spectrum $S(f)$ between $f_{lo,i}$ and $f_{hi,i}$:

$$L_{p,i} = 10 \log_{10} \int_{f_{\text{lo},i}}^{f_{\text{hi},i}} S(f)\, \mathrm{d}f \text{ dB}\,. \tag{C-6}$$

Summing the sound pressure level of all the bands yields the broadband sound pressure level:

$$\text{Broadband SPL} = 10 \log_{10} \sum_i 10^{\frac{L_{p,i}}{10}} \text{ dB}\,. \tag{C-7}$$

Figure C-3 shows an example of how the decidecade band sound pressure levels compare to the sound pressure spectral density levels of an ambient sound signal. Because the decidecade bands are wider than 1 Hz, the decidecade band SPL is higher than the spectral levels at higher frequencies. Decidecade band analysis can be applied to continuous and impulsive sound sources. For impulsive sources, the decidecade band SEL is typically reported.

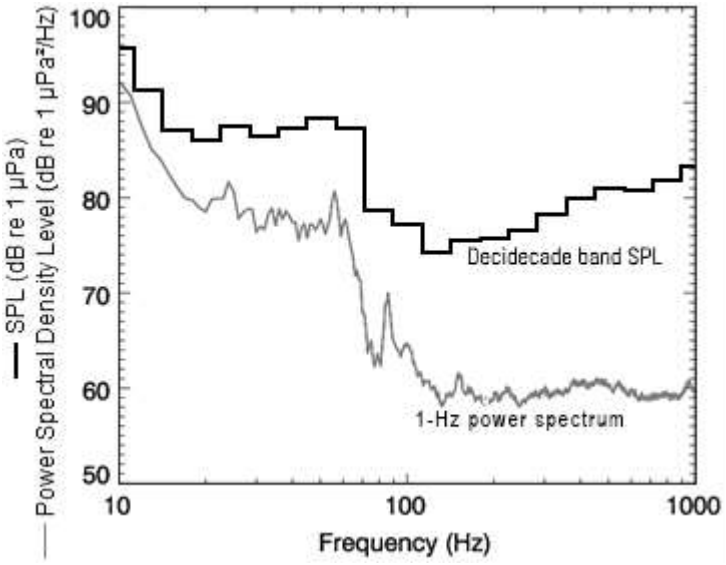

Figure C-3. Sound pressure spectral density levels and the corresponding decidecade band sound pressure levels of a notional ambient sound shown on a logarithmic frequency scale. Because the decidecade bands are wider with increasing frequency, the decidecade band SPL is higher than the power spectrum, which is based on bands with a constant width of 1 Hz.

Table C-1. Decidecade band centre and limiting frequencies (Hz).

Band	Lower frequency	Nominal centre frequency	Upper frequency	Band	Lower frequency	Nominal centre frequency	Upper frequency
10	8.9	10.0	11.2	26	355	398	447
11	11.2	12.6	14.1	27	447	501	562
12	14.1	15.8	17.8	28	562	631	708
13	17.8	20.0	22.4	29	708	794	891
14	22.4	25.1	28.2	30	891	1000	1122
15	28.2	31.6	35.5	31	1122	1259	1413
16	35.5	39.8	44.7	32	1413	1585	1778
17	44.7	50.1	56.2	33	1778	1995	2239
18	56.2	63.1	70.8	34	2239	2512	2818
19	70.8	79.4	89.1	35	2818	3162	3548
20	89.1	100.0	112.2	36	3548	3981	4467
21	112	126	141	37	4467	5012	5623
22	141	158	178	38	5623	6310	7079
23	178	200	224	39	7079	7943	8913
24	224	251	282	40	8913	10000	11220
25	282	316	355	41	11220	12589	14125

Table C-2. Decade band centre and limiting frequencies (Hz).

Decade band	Lower frequency	Nominal centre frequency	Upper frequency
2	10	50	100
3	100	500	1000
4	1,000	5,000	10,000

Appendix D. Sound Propagation Modelling

D.1. MONM-BELLHOP

Underwater sound propagation was predicted for frequencies from 10 Hz to 1.25 kHz with JASCO's Marine Operations Noise Model (MONM). MONM computes acoustic propagation via a wide-angle parabolic equation solution to the acoustic wave equation (Collins 1993) based on a version of the US Naval Research Laboratory's Range-dependent Acoustic Model (RAM), which has been modified to account for a solid seabed (Zhang and Tindle 1995). The parabolic equation method has been extensively benchmarked and is widely employed in the underwater acoustics community (Collins et al. 1996). MONM accounts for the additional reflection loss at the seabed, which results from partial conversion of incident compressional waves to shear waves at the seabed and sub-bottom interfaces, and it includes wave attenuations in all layers. MONM incorporates the following site-specific environmental properties: a bathymetric grid of the modelled area, underwater sound speed as a function of depth, and a geoacoustic profile based on the overall stratified composition of the seafloor. Results from MONM were supplemented with results from the BELLHOP Gaussian beam acoustic ray-trace model (Porter and Liu 1994) for frequencies above 1.25 kHz. BELLHOP accounts for sound attenuation due to energy absorption through ion relaxation and viscosity of water in addition to acoustic attenuation due to reflection at the medium boundaries and internal layers (Fisher and Simmons 1977). The former type of sound attenuation is important for frequencies higher than 5 kHz and cannot be neglected without noticeably affecting the model results.

MONM-BELLHOP computes acoustic fields in three dimensions by modelling transmission loss within two-dimensional (2-D) vertical planes aligned along radials covering a 360° swath from the source, an approach commonly referred to as $N \times$2-D. These vertical radial planes are separated by an angular step size of $\Delta\theta$, yielding $N = 360°/\Delta\theta$ number of planes (left panel, Figure D-1E-1). MONM-BELLHOP treats frequency dependence by computing acoustic transmission loss at the centre frequencies of decidecade bands. Sufficiently many decidecade frequency-bands, starting at 10 Hz, are modelled to include most of the acoustic energy emitted by the source. At each centre frequency, the transmission loss is modelled within each of the N vertical planes as a function of depth and range from the source. The decidecade received SPLs are computed by subtracting the band transmission loss values from the source level in that frequency band. Composite broadband levels are then computed by summing the received decidecade levels. The received sound field within each vertical radial plane is sampled at various ranges from the source, generally with a fixed radial step size (Δr in Figure D-1). At each sampling range along the surface, the sound field is sampled at various depths (Δd in Figure D-1E-1), with the step size between samples increasing with depth below the surface. The received SPL can then be taken at a specific receiver depth or as the maximum value that occurs over all samples within the water column, i.e., the maximum-over-depth received SPL (right panel, Figure D-1E-1).

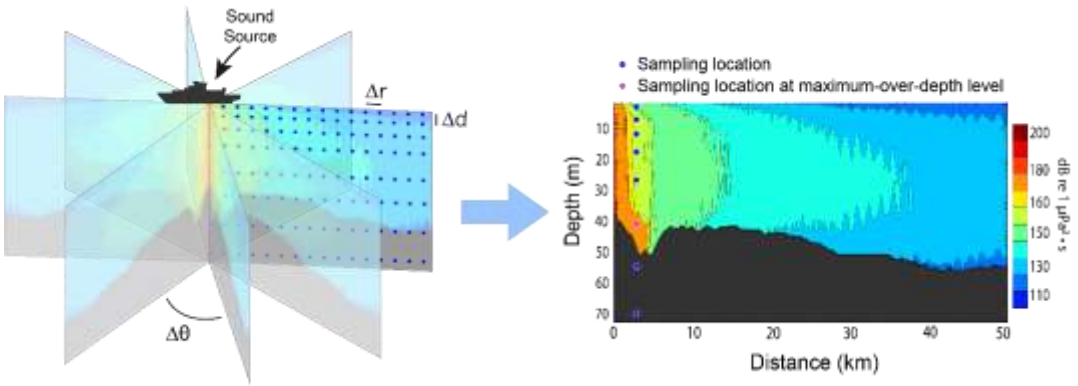

Figure D-1. Representation of $N \times$2-D and maximum-over-depth approaches.

D.2. Estimating Ranges to Threshold Levels

Sound level contours were calculated based on the underwater sound fields predicted by the propagation models, sampled both at the seafloor as well as by taking the maximum value over all modelled depths above the seafloor for each location in the modelled region. The predicted distances to specific levels were computed from these contours. Two distances relative to the source are reported for each sound level: (1) R_{max}, the maximum range to the given sound level over all azimuths, and (2) $R_{95\%}$, the range to the given sound level after the 5% farthest points were excluded (see examples in Figure D-2E-2).

The $R_{95\%}$ is used because sound field footprints are often irregular in shape. In some cases, a sound level contour might have small protrusions or anomalous isolated fringes. This is demonstrated in the image in Figure D-2a. In cases such as this, where relatively few points are excluded in any given direction, R_{max} can misrepresent the area of the region exposed to such effects, and $R_{95\%}$ is considered more representative. In contrast, in strongly radially asymmetric cases such as shown in Figure D-2b, $R_{95\%}$ neglects to account for substantial protrusions in the footprint. In such cases, R_{max} might better represent the region of effect in specific directions. Cases such as this are usually associated with bathymetric features that affect propagation. The difference between R_{max} and $R_{95\%}$ depends on the source directivity and the non-uniformity of the acoustic environment.

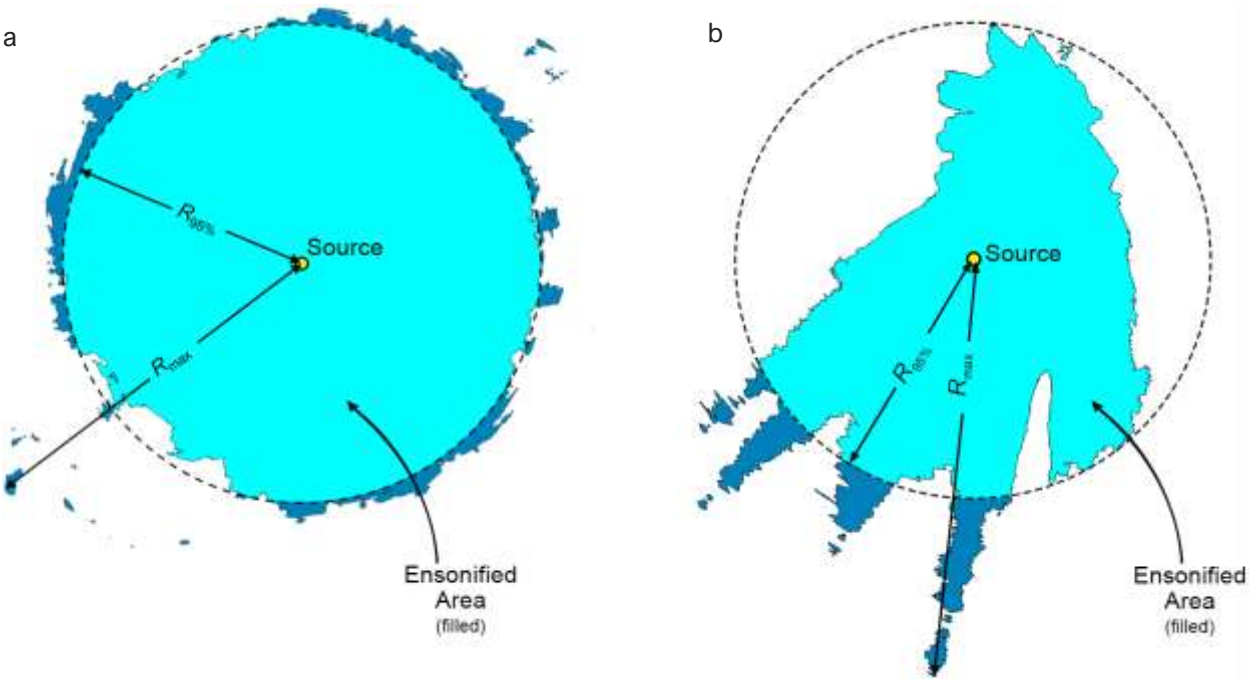

Figure D-2. Sample areas ensonified to an arbitrary sound level with R_{max} and $R_{95\%}$ ranges shown for two contrasting scenarios: (a) a largely radially symmetric sound level contour with small protrusions, for which $R_{95\%}$ best represents the ensonified area; and (b) a strongly asymmetric sound level contour with long protrusions, for which R_{max} best represents the ensonified areas in some directions. Light blue indicates the ensonified areas bounded by $R_{95\%}$; darker blue indicates the ensonified areas beyond $R_{95\%}$ that determine R_{max}.

Appendix E. Supplementary Modelling Materials

E.1. Decidecade Source Levels

Table E-1. Decidecade band source levels for the various vessel types.

Band Centre Frequency (Hz)	Decidecade Band Source Level (dB re 1 µPa·m)					
	LLS – S	LLS – M	LLS – L	OTB – S	OTB – M	OTB – L
10	126.3	128.5	129.7	161.8	163.9	165.7
13	127.3	129.5	130.8	166.6	168.7	170.5
16	128.3	130.5	131.8	159.8	161.9	163.7
20	129.3	131.6	132.8	161.7	163.8	165.6
25	130.4	132.6	133.9	160.4	162.5	164.3
32	131.4	133.7	134.9	159.9	162.0	163.8
40	132.5	134.7	136.0	161.4	163.5	165.3
50	133.5	135.8	137.0	166.6	168.7	170.5
63	134.6	136.8	138.1	164.6	166.7	168.5
79	135.6	137.8	139.1	158.1	160.2	162.0
100	136.5	138.8	140.0	157.3	159.4	161.2
126	137.4	139.6	140.9	151.7	153.8	155.6
158	138.0	140.3	141.5	155.3	157.4	159.2
200	138.4	140.7	141.9	159.1	161.2	163.0
251	138.5	140.7	142.0	155.3	157.4	159.2
316	138.3	140.5	141.8	154.6	156.7	158.5
398	137.7	140.0	141.2	150.4	152.5	154.3
501	137.0	139.2	140.5	156.0	158.1	159.9
631	136.1	138.3	139.6	158.7	160.8	162.6
794	135.1	137.3	138.6	162.8	164.9	166.7
1000	134.1	136.3	137.5	156.2	158.3	160.1
1259	133.0	135.2	136.5	155.2	157.3	159.1
1585	132.0	134.2	135.4	154.1	156.2	158.0
1995	130.9	133.1	134.4	153.1	155.2	156.9
2512	129.9	132.1	133.3	152.0	154.1	155.9
3162	128.8	131.0	132.3	151.0	153.1	154.9
3981	127.8	130.0	131.3	150.0	152.1	153.8
5012	126.8	129.0	130.2	148.9	151.0	152.8
6310	125.7	128.0	129.2	147.9	150.0	151.8
7943	124.7	126.9	128.2	146.9	149.0	150.8
10000	123.7	125.9	127.2	145.9	148.0	149.7
12589	122.7	124.9	126.2	144.9	147.0	148.7
15849	121.7	123.9	125.2	143.8	145.9	147.7
19953	120.7	122.9	124.2	142.8	144.9	146.7
25119	119.7	121.9	123.1	141.8	143.9	145.7

E.2. Multiple Vessel Scenario Source Locations

The vessel types modelled at each location for the multiple vessel scenarios are presented graphically in Figures E-1 to E-3. The types of vessel and source locations in Zone B are the same for Scenarios 1 and 2.

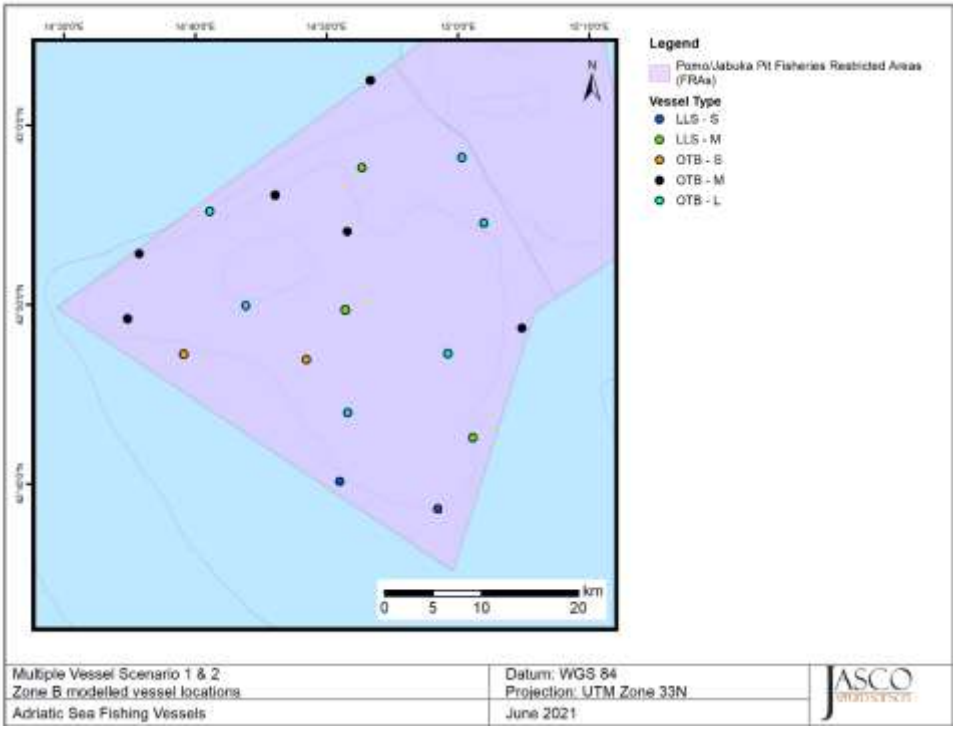

Figure E-1. Modelled source locations in Zone B for multiple vessel Scenarios 1 and 2.

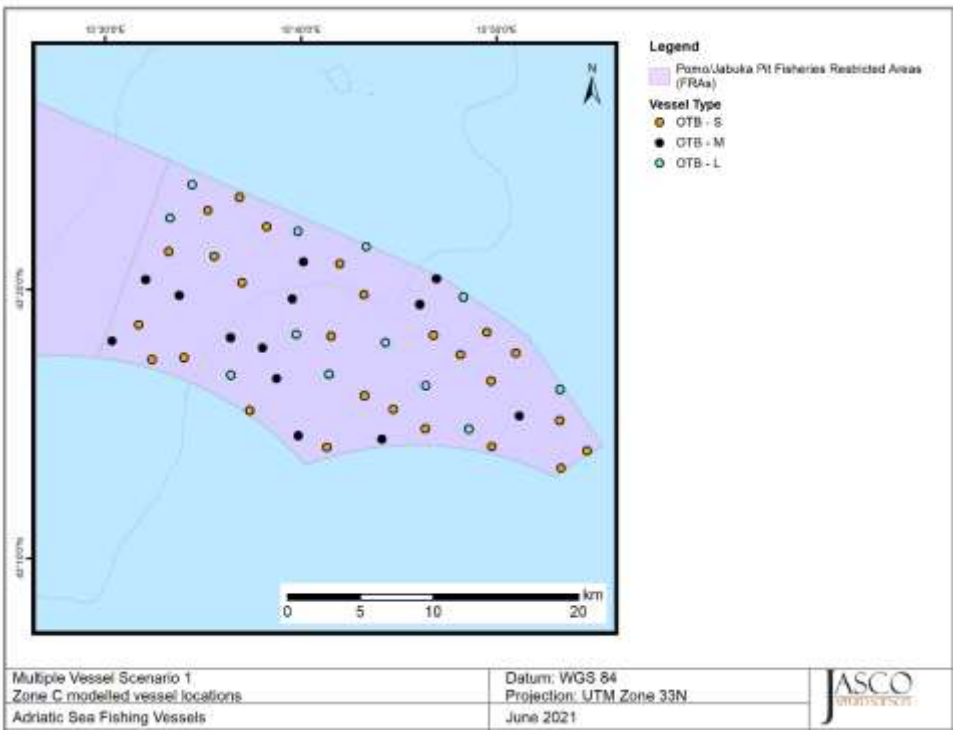

Figure E-2. Modelled source locations in Zone C for multiple vessel Scenario 1.

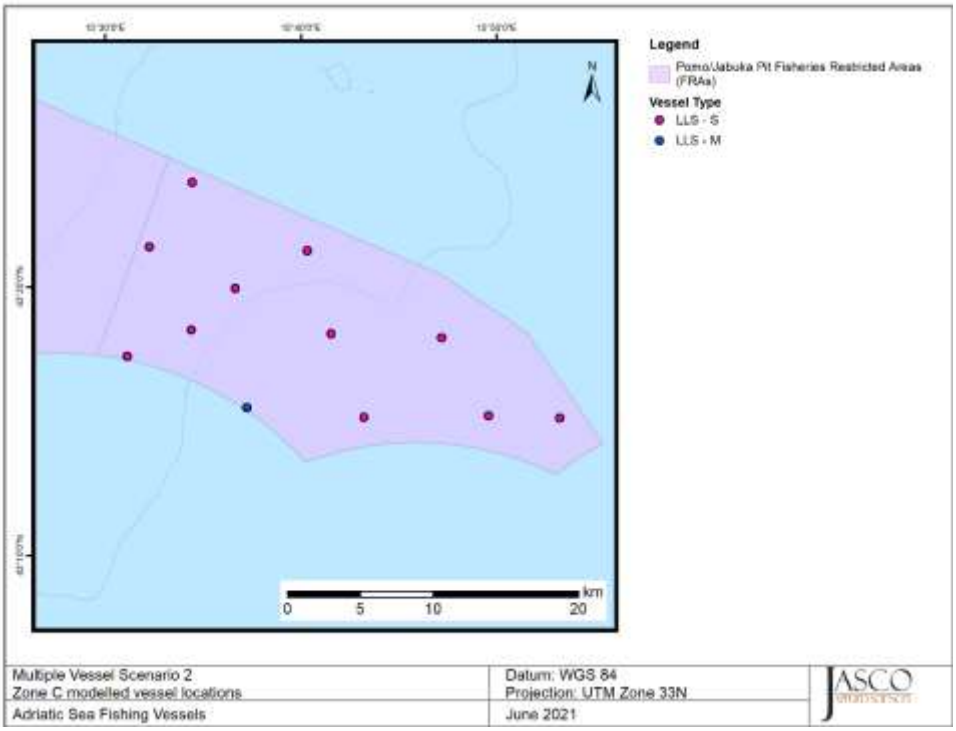

Figure E-3. Modelled source locations in Zone C for multiple vessel Scenario 2.